

Neurobiology

Elevated Neuronal Expression of CD200 Protects *Wld^s* Mice from Inflammation-Mediated Neurodegeneration

Tanuja Chitnis,* Jaime Imitola,* Yue Wang,*

Wassim Elyaman,* Prianka Chawla,*

Maia Sharuk,* Khadir Raddassi,*

Roderick T. Bronson,[†] and Samia J. Khouri*

From the Center for Neurologic Diseases,* Brigham and Women's Hospital, Boston; and the Rodent Histopathology Core Facility,[†] Dana-Farber/Harvard Cancer Center, Department of Pathology, Harvard Medical School, Boston, Massachusetts

Axonal damage secondary to inflammation is likely the substrate of chronic disability in multiple sclerosis and is found in the animal model of experimental autoimmune encephalomyelitis (EAE). *Wld^s* mice have a triplication of the fusion gene *Ube4b/Nmnat* and a phenotype of axon protection. *Wld^s* mice develop an attenuated disease course of EAE, with decreased demyelination, reduced axonal pathology, and decreased central nervous system (CNS) macrophage and microglial accumulation. We show that attenuated disease in *Wld^s* mice was associated with robust constitutive expression of the nonsignaling CD200 molecule on neurons in the CNS compared with control mice. CD200 interacts with its signaling receptor CD200R, which we found to be expressed on microglia, astrocytes, and oligodendrocytes at similar levels in control and *Wld^s* mice. Administration of blocking anti-CD200 antibody to *Wld^s* mice abrogated disease attenuation and was associated with increased CNS inflammation and neurodegeneration. *In vitro*, *Wld^s* neuronal cultures were protected from microglial-induced neurotoxicity compared with control cultures, but protection was abrogated by anti-CD200 antibody. The CD200-CD200R pathway plays a critical role in attenuating EAE and reducing inflammation-mediated damage in the CNS. Strategies that up-regulate the expression of CD200 in the CNS or molecules that ligate the CD200R may be relevant as neuroprotective strategies in multiple sclerosis. (Am J Pathol 2007; 170:1695–1712; DOI: 10.2353/ajpath.2007.060677)

Multiple sclerosis (MS) is an immune-mediated demyelinating and degenerative disease of the central nervous system (CNS). Axonal damage and demyelination are present in both MS and its animal model, experimental autoimmune encephalomyelitis (EAE), and are implicated as the primary determinants of irreversible neurological deficits.^{1,2} Axonal damage is a consequence of both immune-mediated damage as well as activation of degenerative pathways; however, the underlying mechanisms are not well understood.

The *Wld^s* mouse is a spontaneously occurring mutant with the unique phenotype of protection against several forms of axonal injury. Degeneration of the distal portion of the axon or Wallerian degeneration has been shown to be delayed in the *Wld^s* mouse after both peripheral^{3,4} and CNS nerve transections.⁵ In addition, axons have been shown to remain viable after apoptosis of the neuronal cell body.⁶ The *Wld^s* gene has also been shown to be protective in models of vincristine- and paclitaxel-induced neuropathy, suggesting that it has multifaceted neuroprotective effects.^{7,8} Several studies have demonstrated reduced microglial responses after axonal transection in the *Wld^s* model.^{9–13} Experiments using bone marrow chimaeras have proven that this is a property that affects "cell populations intrinsic to the *Wld^s* nerve and is not attributable to an anomaly in circulating monocytes."¹⁴

We have recently shown that compared with wild-type (WT) mice, *Wld^s* mice, when immunized to induce chronic EAE, developed a delayed onset and an attenuated disease course,¹⁵ which was associated with a reduction in both axonal loss and demyelination in spinal cord sections. Axonal protection in *Wld^s* mice was associated with

Supported by the National Institutes of Health (grants AI058680 and AI043496 to S.J.K. and National Institute of Neurological Disorders and Stroke grant KO8 NS 047669-01 to T.C.) and the National Multiple Sclerosis Society (Pilot Project grant to T.C. and grants RG3666 and RG2988 to S.J.K.).

Accepted for publication January 16, 2007.

Address reprint requests to Tanuja Chitnis, M.D., 77 Avenue Louis Pasteur, Room 714, Center for Neurologic Diseases, Brigham and Women's Hospital, Boston, MA 02115. E-mail: tchitnis@rics.bwh.harvard.edu.

increased nicotinamide adenine dinucleotide (NAD) levels; however, the molecular mechanisms mediating axon protection in *Wld^s* mice have not been elucidated. In this study, we explored molecular mediators of neuroprotection in the *Wld^s* EAE model with the goal of identifying potential therapeutic targets for MS. Although there was no difference in T-cell infiltrates in the CNS,¹⁵ we found that microglia and macrophage accumulation and activation in the CNS were diminished in *Wld^s* mice compared with WT mice. Microglia and macrophages have been associated with axonal damage within MS lesions,¹⁶ as well as in diffuse axonal damage in the normal appearing white matter.¹⁷ Because of these observations, we explored the differential expression of molecules associated with microglial regulation.

We found that disease protection in *Wld^s* mice as well as in neuronal cultures was associated with enhanced neuronal and glial expression of CD200, a nonsignaling molecule that has previously been described on neurons^{18–20} and belongs to the immunoglobulin superfamily of glycoproteins. Interaction of CD200 with its ligand, CD200R, has been shown to initiate tyrosine phosphorylation.²¹ Thus, the effects of CD200 are mediated through cells expressing the CD200 receptor (CD200R), including microglia/macrophages.^{21–23} Macrophage/microglial responses to nerve trauma and EAE were accelerated in mice deficient for CD200.²⁴ These and other studies²⁵ suggest that ligation of CD200R delivers a negative signal for microglia/macrophage activation. CD200R has been found to also be expressed on dendritic cells, mast cells, granulocytes, and to a limited extent on CD8⁺ T cells, natural killer (NK) cells, NKT cells, and CD4⁺ cells of the Th2 phenotype.²³ Four isoforms of CD200R have been described, and at least in one study, all four have been shown to bind CD200.²⁶ More recently CD200R agonists have been shown to inhibit proinflammatory cytokine secretion by macrophage cell lines, including interleukin (IL)-17-induced IL-6 production.²⁷ CD200R ligation on mast cells inhibits degranulation and cytokine production.²⁸ CD200R ligation induces regulatory dendritic cell populations capable of secreting indolamine dioxygenase.²⁹ Moreover, in animal models, CD200R agonists have been shown to ameliorate collagen-induced arthritis³⁰ and prolong graft survival.³¹

Using the *Wld^s* model, we studied the effects of neuronal CD200 overexpression in models of inflammation-induced neurotoxicity. We show that increased expression of CD200 is capable of protecting neurons and axons from microglia-induced damage *in vitro* and *in vivo*. Moreover, we demonstrated that the CD200 receptor is expressed on CNS glial cells as well as peripheral splenocytes, suggesting that the CD200-CD200R pathway can play a regulatory role in both the CNS and the periphery. Thus, strategies to enhance the CNS expression of CD200 or to ligate its receptor may suppress inflammation-mediated neurodegeneration present in diseases including multiple sclerosis.

Materials and Methods

Animals

Female C57BL/6O1aHSD-*Wld^s* and wild-type C57BL/6O1aHSD (WT) from Harlan UK Limited (Bicester, Oxon, UK) were obtained for EAE studies. C57BL/6O1aHSD-*Wld^s* mice are homozygous mutants. Mice were 6 to 10 weeks old at the time of immunization.

Induction of EAE, Scoring, and Analysis of Clinical Disease

Myelin oligodendrocyte glycoprotein peptide 35-55 (MOG 35-55) (MEVGWYRSPFSRVVHLYRNGK) corresponding to mouse sequence was synthesized by QCB Inc. (Division of BioSource International, Hopkinton, MA) and purified to >99% by high-performance liquid chromatography. Mice were immunized with 150 µg/75 µl of MOG peptide emulsified with an equal volume of complete Freund's adjuvant containing *Mycobacterium tuberculosis* (H37RA; Difco, Detroit, MI) at a final concentration of 2 mg/ml. Two hundred ng of pertussis toxin was injected intraperitoneally (List Laboratories, Campbell, CA) on day 0 and day 2 after immunization. EAE was scored by a blinded observer on a scale from 0 to 5, as previously described³²: grade 1, limp tail or isolated weakness of gait without limp tail; grade 2, partial hind leg paralysis; grade 3, total hind leg or partial hind and front leg paralysis; grade 4, total hind leg and partial front leg paralysis; and grade 5, moribund or dead animal.

A subgroup of *Wld^s* and WT mice were treated with 200 µg/100 µl of blocking anti-CD200 antibody (clone 10A5, anti-mouse-CD200 rat IgG1κ; Trillium Therapeutics Inc., Toronto, ON, Canada)^{25,30} injected intravenously every other day from days 10 to 20. Control WT and *Wld^s* mice were treated with phosphate-buffered saline (PBS) alone or rat IgG control (Sigma, St. Louis, MO).

Delayed-Type Hypersensitivity

Delayed-type hypersensitivity responses were assessed by the measurement of ear thickness using calipers (IDC series 543; Mitutoyo, Tokyo, Japan), 48 hours after intra-dermal injection with MOG peptide (50 µg in 50 µl of PBS) in one ear and an equal volume of PBS in the contralateral ear. Results were reported as fold change in ear thickness of MOG-injected ear/PBS-injected ear. Results from four to six mice per strain were averaged.

Preparation of Tissue for Histology Studies

Mice were euthanized using CO₂ and perfused with PBS followed by 4% paraformaldehyde or Bouin's solution (Electron Microscopy Sciences, Fort Washington, PA). Spinal cords and brains were collected at specified time points, using three to four mice in each experimental group. For paraffin embedding, tissues were stored in Bouin's solution for minimum of 48 hours, and paraffin sections were prepared. For immunofluorescence stain-

ing, tissues were kept in 4% paraformaldehyde for 48 hours, placed in a 30% sucrose gradient, and then embedded in O.C.T. (Electron Microscopy Sciences), quick-frozen in liquid nitrogen and stored at -80°C until sectioning.

Bielschowsky Staining

Sections cut from paraffin-embedded tissue, were placed in a 20% silver nitrate solution at 37°C. Sections were washed in ammonia, and then a developer solution was added for 3 to 5 minutes until sections were black. Slides were rewashed in ammonia water, dH₂O, fixed in 5% thiosulfate for 1 minute, washed, dehydrated, and then mounted in Permount.

Luxol Fast Blue Staining

Sections were cut from paraffin-embedded tissue. Slides were placed in Luxol fast blue solution overnight at 55°C, differentiated in alcohol, dipped in 0.05% lithium carbonate solution, and then counterstained with cresyl violet.

Axon Loss and Demyelination Quantification

Axon loss and demyelination were quantified as follows. Transverse spinal cord sections at the cervical, thoracic, and lumbar levels from WT and *Wld^s* mice at day 60 after immunization were stained with Bielschowsky or Luxol fast blue, as described. Photomicrographs ($\times 100$) were taken of sections from the anterior, lateral, and posterior sections of each spinal cord level, using specific landmarks for orientation. The area of regions with >50% axon density or demyelinated areas were quantified, and percent axon loss or demyelination was calculated in comparison to total white matter per section using the NIH Image Analyzer program (Bethesda, MD).

Immunofluorescence Technique

Using perfused frozen sections mounted in O.C.T., 30- μ m free-floating sections were cut using a cryotome. Sections were blocked in PBS containing 4% goat serum, 0.3% bovine serum albumin, and 0.3% Triton X-100 and incubated with primary antibodies at 4°C overnight, followed by fluorescein- or rhodamine-labeled secondary antibodies 1:250 to 1:500 (Molecular Probes, Eugene, OR) for 2 hours in blocking solutions.

Antibodies Used for Immunofluorescence Staining

The following antibodies were used: CD200 (clone 3B6, isotype rat IgM, 1:200; Cedarlane Laboratories, Hornby, ON, Canada); secondary: Alexa 488-conjugated goat anti-rat IgM (Molecular Probes); CD200R (anti-313015 CD200R peptide,²⁶ clone R252, isotype rabbit IgG, 1:200; Trillium Therapeutics Inc.); secondary: Alexa 594-conjugated goat anti-rabbit IgG (Molecular Probes);

CD200R (clone OX-110, isotype rat IgG2a, 1:100; Serotec, Oxford, UK); secondary: Alexa 488-conjugated rabbit anti-rat IgG (Molecular Probes); mitogen-activated protein 2 (MAP-2) (clone HM-2: mouse anti-mouse IgG1, 1:100; Sigma); secondary: Alexa 594-conjugated goat anti-mouse IgG (Molecular Probes); NeuN (clone A60, isotype mouse IgG1, 1:100; Chemicon/Millipore, Temecula, CA); secondary: Alexa 594-conjugated goat anti-mouse IgG (Molecular Probes); GFAP cocktail (clones 4A11, 1B4, 2E1, isotype mouse IgG2b, 1:100; BD Pharmingen, Palo Alto, CA); secondary: Alexa 488- or Alexa 594-conjugated goat anti-mouse IgG (Molecular Probes); CNPase (clone 11-5B, isotype mouse IgG1, 1:100; Chemicon/Millipore); secondary: Alexa 488- or Alexa 594-conjugated goat anti-mouse IgG (Molecular Probes); β -tubulin (clone TUJ1, isotype mouse IgG2a; 1:100; Covance, Berkeley, CA); secondary: Alexa 488- or Alexa 594-conjugated goat anti-mouse IgG (Molecular Probes); CD4 (clone H29.129; isotype rat IgG2a; 1:50; BD Pharmingen); secondary: Alexa-488-conjugated goat anti-rat IgG (Molecular Probes); and CD8 (clone 53-6.7; isotype rat IgG2a, 1:50; BD Pharmingen); secondary: Alexa-488-conjugated goat anti-rat IgG (Molecular Probes). The following isotype controls were used: rabbit polyclonal IgG isotype control (Abcam Inc., Cambridge, MA), rat IgG2a isotype control (eBioscience, San Diego, CA), mouse IgG1 isotype control (eBioscience), mouse IgG2a isotype control (eBioscience), and mouse IgG2b isotype control (eBioscience).

Lectin B4 Immunofluorescent Staining

Spinal cord sections from WT and *Wld^s* mice were incubated with fluorescein isothiocyanate (FITC)-conjugated *Griffonia simplicifolia* isolectin B4 (LB4) 1:100 (Vector Laboratories, Burlingame, CA) using the standard immunofluorescence protocol described above. Secondary reagent Alexa 488-conjugated anti-FITC antibody (1:500) (Molecular Probes) was used to visualize LB4 staining. Two spinal cord sections from each of five mice per strain per time point were stained for LB4 (for a total of 10 sections per strain per time point). The number of CD4⁺ or CD8⁺ LB4⁺ foci in five adjacent fields per section was quantified. Perimeningeal foci were defined as those limited to the meninges or subpial region, whereas parenchymal foci were defined as those beyond the subpial region.

Confocal Microscopy

Confocal microscopy was performed using a Zeiss LSM equipped with argon-Kr/HeNe lasers (Zeiss, Heidelberg, Germany), and Zeiss 3D analysis software. Three-dimensional images were obtained using Z-series stacking.

Electron Microscopy

Animals with EAE and naïve animals were perfused and fixed with 2.5% paraformaldehyde/2.5% glutaraldehyde solution in 0.1 mol/L sodium cacodylate. The spinal cord

was postfixed, dehydrated through serial ethanol concentrations, and embedded in EPON. Thick sections were stained with toluidine blue and examined for regions of interest. Sections were thin cut (1 μm), stained with 2% uranyl acetate in 0.1 mol/L sodium acetate, and followed by lead citrate. Sections were then placed on a carbon-coated formvar grid and viewed with a Hitachi 600 transmission electron microscope (Harvard EM Facility).

Proliferation Assay and Cytokine Enzyme-Linked Immunosorbent Assay (ELISA)

For proliferation and cytokine measurement, splenocytes were cultured in 96-well plates (Costar, Cambridge, MA). Media used for proliferation and cytokine assays consisted of serum-free Dulbecco's modified Eagle's medium (BioWhittaker, Walkersville, MD) containing 75 mmol/L/ml L-glutamine, 100 U/ml penicillin and streptomycin, 1 ml/100 ml of media of a 100 \times concentrated nonessential amino acid solution, 0.1 mmol/L HEPES/ml, 1 mmol/L/ml sodium pyruvate (all BioWhittaker), and 0.05 mmol/L/ml 2-mercaptoethanol (Sigma). Cells were incubated at 37°C in humidified air containing 7% CO₂.

Proliferation Assay

For proliferation assay, cells were cultured at 2 \times 10⁶ cells/ml and 200 μl /well with various antigen concentrations. After 48 hours of culture, 1 μCi of [³H]thymidine (NEN, Boston, MA) was added in 10 μl of media to each well for another 16 hours. Cells were harvested on filter mats, dried, and counted.

Cytokine ELISA

For ELISA, cytokine assay cells were cultured at 4 \times 10⁶ cells/ml in 200 μl of media at various antigen concentrations. Supernatants for ELISA were collected after 48 hours of culture. Quantitative ELISAs for IL-5, IL-6, IL-10, and interferon (IFN)- γ were performed on 96-well Nunc-Immuno plates (Nalge Nunc International, Rochester, NY) using paired antibodies and recombinant cytokines from Pharmingen, according to the manufacturer's recommendations.

Flow Cytometric Analysis of Splenocytes

Splenocytes from either wild-type or *Wld^s* mice were washed and resuspended in PBS to a concentration of 10⁷ cells/ml. Cells were incubated on ice with 5 $\mu\text{g}/10^6$ cells of the appropriate cellular marker (phycoerythrin-conjugated; Pharmingen) and 5 $\mu\text{g}/10^6$ of rat anti-mouse CD200 FITC-conjugated antibody (Cedarlane Laboratories) or anti-CD200R1 FITC-conjugated antibody (Serotec) when indicated for 20 minutes on ice. Cells were then washed and analyzed by flow cytometry on a FACScan (Becton Dickinson Immunocytometry Systems, San Jose, CA). The percentage of double-positive cells per sample group was calculated.

Flow Cytometric Analysis of Spinal Cord Homogenates

Mice were sacrificed and perfused intracardially with 20 ml of ice-cold PBS. Spinal cords were isolated and passed through a 70- μm nylon filter, spun down, and resuspended in Hanks' balanced salt solution with 10 mmol/L HEPES and 2 mmol/L ethylenediaminetetraacetic acid and incubated on a rotating shaker for 1 hour at 4°C. The pellet was resuspended in 5 ml of isotonic 37% Percoll and spun down. The supernatant was removed, and the pellet was resuspended in PBS containing 1% bovine serum albumin for flow cytometric studies. Antibodies used for flow cytometric studies included FITC- or phycoerythrin-conjugated antibodies to CD11b, CD4, CD8, CD11c, NK1.1, TCR $\alpha\beta$, CD19, Gr1, and allophycocyanine-conjugated CD45 as well as isotype controls (Pharmingen). Allophycocyanine-conjugated FoxP3 antibody was obtained from eBioscience.

Immunoblotting

Tissues were dissected and homogenized in lysis buffer [25 mmol/L Tris-HCl, pH 7.4, 150 mmol/L NaCl, 1 mmol/L ethylenediaminetetraacetic acid, 0.5% Triton X-100, 10% glycerol, and one tablet of protease inhibitors (Boehringer, Indianapolis, IN)]. Lysates were centrifuged, the resulting supernatants were collected, and protein concentrations were determined by bicinchoninic acid assay (Pierce, Rockford, IL). Samples were mixed with 3 \times Laemmli's buffer and heated at 99°C for 5 minutes, and equal amounts of total protein was loaded onto 4 to 20% sodium dodecyl sulfate-polyacrylamide gel electrophoresis and transferred to nitrocellulose membranes. Blots were probed for 2 hours at room temperature or overnight at 4°C with primary monoclonal antibodies CD200 (1:10,000) and β -actin (1:5000), rinsed in phosphate-buffered saline/Tween 20, incubated for 1 hour at room temperature with horseradish peroxidase-conjugated goat anti-mouse (Santa Cruz Biotechnology, Inc., Santa Cruz, CA) (1:10,000) or anti-rat antibodies (Caltag, Burlingame, CA) (1:10,000). Membranes were washed in Tris-buffered saline/Tween 20, and immunoreactive proteins were detected using the enhanced chemiluminescence method (Amersham, Piscataway, NJ). Immunoreactivity was quantified using the NIH Image analyzer program.

Immunoprecipitation

Spinal cord lysates from WT and *Wld^s* mice were incubated with anti-CD200 antibody for 18 hours at 4°C, immunoprecipitated with protein G agarose suspension, and separated on 10% polyacrylamide gel. Samples were immunoblotted with either ubiquitin or CD200 using the same protocol described above. CD22 expression in spinal cord lysates was assessed by immunoblot using anti-CD22 antibody (clone MYG13; Santa Cruz Biotechnology).

CNS Fractalkine (CX3CL1) Expression by ELISA Assay

We followed the protocol outlined by Huang and colleagues.³³ Spinal cords were manually homogenized in 1 ml of lysis buffer (150 mmol/L NaCl, 0.01 mol/L Tris, 1.0 mmol/L ethylenediaminetetraacetic acid, 1.0 µg/ml aprotinin, and 100 µg/ml phenylmethyl sulfonyl fluoride) and centrifuged at 500 × g for 10 minutes. Protein concentration in the supernatants was measured, and four samples per group, each containing 2.0 µg/ml total protein in 50 µl of PBS, were assayed for fractalkine concentration using a fractalkine ELISA assay (DY472; R&D Systems Inc., Minneapolis, MN), which contains anti-CX3CL1 and conjugated anti-CX3CL1, as well as a recombinant fractalkine standard.

Primary Microglia Culture Preparation

Cortices were dissected from P1 C57BL/6 mice, and trypsin was added for 15 minutes, followed by dissociation by trituration through a fire-polished pipette. Cells were counted and 12 × 10⁶ cells were diluted in Dulbecco's modified Eagle's medium (Life Technologies, Inc., Carlsbad, CA) supplemented with 10% fetal bovine serum and 1% penicillin/streptomycin were placed in T75 flasks precoated overnight with poly-L-lysine. After 10 days, cells were labeled with anti-CD11b antibody and sorted using a Cell Sorter (FACSVantage, SE Cell Sorter; BD Biosciences, Franklin Lakes, NJ).

Neuronal Microglia Co-Culture Preparation

Neuronal cultures were prepared as follows. E16-18 cortices were stripped from meningeal tissue on Hanks' balanced salt solution and dissociated with 1 ml of trypsin at 37°C for 15 minutes. Cells were dissociated using a polished Pasteur pipette, counted, and plated at 5 × 10⁴/200 µl per well on poly-L-lysine (Sigma)-coated coverslips (Fisher Scientific, Pittsburgh, PA) in 24-well plates in neurobasal medium containing 2% B27 supplement 1% L-glutamine and 0.5% penicillin/streptomycin at 37°C in humidified air containing 5% CO₂. BV-2 microglial cell line (American Type Culture Collection, Rockville, MD) was cultured in Dulbecco's modified Eagle's medium (Life Technologies, Inc.), supplemented with 10% heat-inactivated fetal bovine serum and 0.5% penicillin-streptomycin and incubated at 37°C in humidified air containing 5% CO₂ until confluent. Microglia (15 × 10³ cells/well) were seeded with primary neuronal cultures and stimulated using lipopolysaccharide (LPS) (0.05 µg/ml) or 1 ng/ml IFN-γ (R&D Systems Inc.) for 48 hours. Anti-CD200 blocking antibody (clone 10A5, anti-mouse-CD200 rat IgG1κ) and CD200-F(Ab')₂ (clone 10A5, anti-mouse-CD200 rat IgG1κ) was supplied to us by Trillium Therapeutics Inc.^{25,30}

Statistical Analysis

For statistical evaluation of clinical course, data were pooled from different experiments. Analysis was performed using Mann-Whitney U-test. P values <0.05 were considered significant.

Results

Wld^s Mice Experience an Attenuated Course of EAE with Delayed Onset of Disease

Wld^s mice and WT C57BL/6 mice were immunized with MOGp35-55 (Figure 1). Clinical disease course was assessed by a blinded observer and scored on a scale from 0 to 5.³² As shown in Table 1, composite analysis of five experiments shows disease onset was significantly delayed in *Wld^s* mice (day of onset = 17.58 ± 9.3) compared with WT mice (day of onset = 10.88 ± 1.45, P = 0.0068; Mann-Whitney test). Disease onset in *Wld^s* mice ranged from day 10 to day 29 after immunization, with 25% of mice experiencing a disease onset later than day 20. Mean maximal grade was significantly lower in *Wld^s* mice during the first 20 days after immunization (*Wld^s* = 0.98 ± 1.19; WT = 2.34 ± 0.72, P = 0.0002), with a trend toward attenuated disease in *Wld^s* mice compared with WT mice, at later time points (Table 1). Figure 1 shows EAE mean disease grade in a composite of animals from all five experiments listed in Table 1.

*Axonal Damage and Demyelination Are Reduced in *Wld^s* Mice during EAE*

To understand the underlying mechanisms of EAE disease attenuation, we performed histopathological analysis of *Wld^s* and WT spinal cords. Vesicular disruption of the myelin sheath and collapsed myelin sheaths devoid of axons were observed in the spinal cords of WT mice, as demonstrated in toluidine blue-stained and electron microscopy sections harvested at day 25 after immunization (Figure 1, b and c). In contrast, both axons as well as myelin sheaths were relatively preserved in *Wld^s* mice harvested at the same time point. In addition, there was a striking paucity of microglia/macrophages in the white matter of *Wld^s* spinal cord sections compared with WT.

Six to eight mice per group were selected for examination of axonal loss and demyelination at day 60 after immunization. The average EAE disease grade for WT mice used for tissue analysis at the time of harvesting was 2.08 ± 0.86, whereas the average score for *Wld^s* mice used was 1.33 ± 0.75 (P = NS; Student's t-test), within the range of disease grades recorded in Table 1. Silver staining of cervical, thoracic, and lumbar sections of the spinal cord demonstrated reduced axonal loss in *Wld^s* mice at all levels of the spinal cord, particularly in the cervical-thoracic cord (Figure 1d). Luxol fast blue staining of adjacent sections showed that demyelination was also significantly reduced at all levels of the spinal cord in *Wld^s* mice (Figure 1e). Total axonal loss was

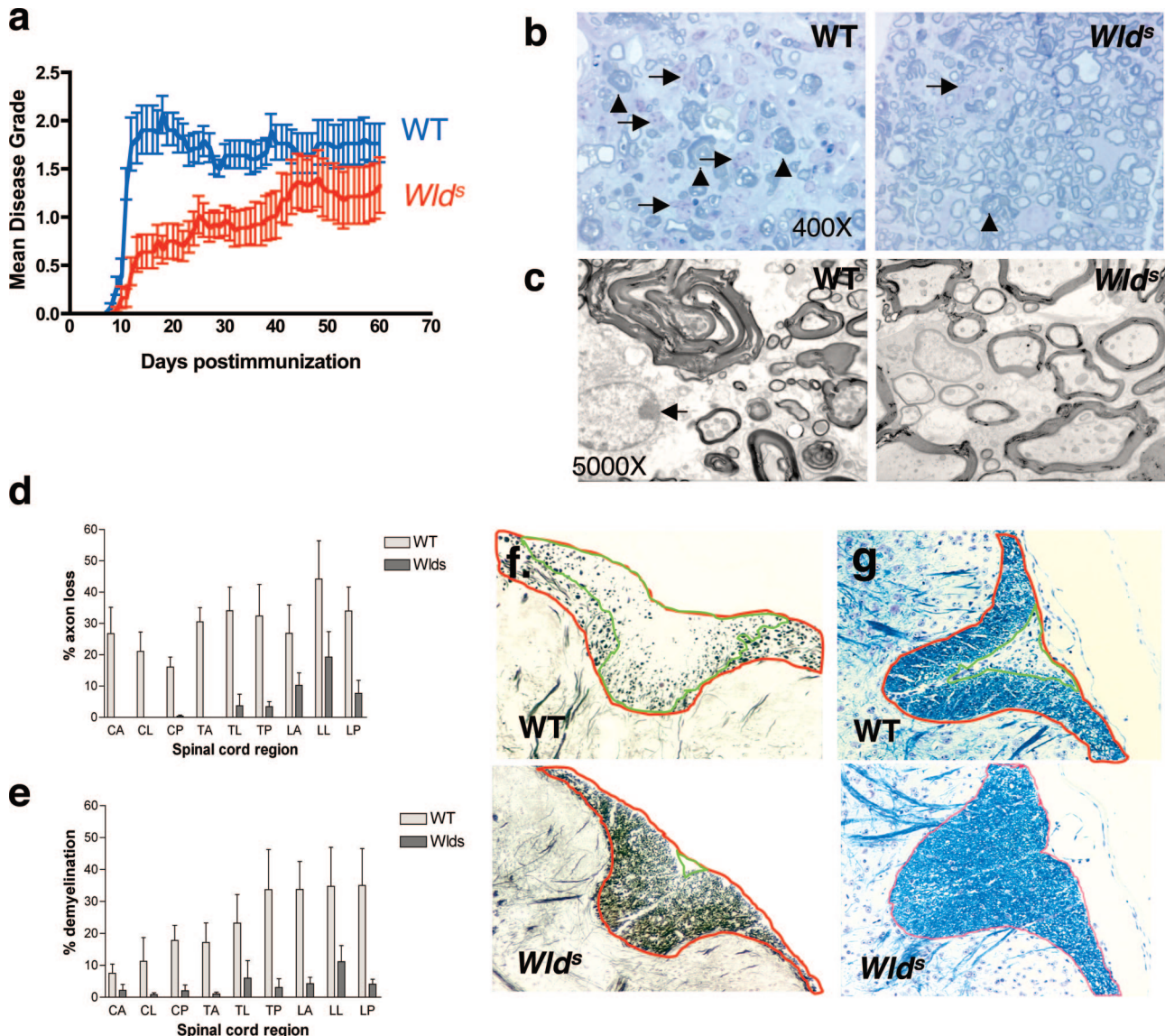


Figure 1. Wld^s mice have an attenuated course of EAE with less axonal loss and demyelination. **a:** Wld^s and WT mice were immunized with 150 μ g of MOGp35-55. EAE disease grade was followed daily from day 0 to 60. Shown is the mean disease grade \pm SE from a composite of five separate experiments (28 Wld^s mice, 16 WT mice). Wld^s mice experience an attenuated course of disease. **b:** Representative toluidine blue-stained sections from the lateral lumbar spinal cord from WT and Wld^s mice on day 25 after immunization show more severe demyelination, axonal loss (**arrowheads**), and general tissue destruction in WT mice. In addition, more macrophages/microglia are present in WT sections (**arrows**). **c:** Electron microscopy sections from the lateral lumbar spinal cord regions from WT and Wld^s mice harvested at day 25 after immunization depict vesicular disruption of myelin sheaths in WT mice only, despite the presence of macrophages in both samples (**arrows**). **d:** Quantification of axonal loss in anterior (A), lateral (L), and posterior (P) sections of Bielschowsky silver-stained sections from cervical (C), thoracic (T), and lumbar (L) levels of the spinal cord from mice at day 60 after immunization. Results from six to eight spinal cords per group are averaged and shown. Average EAE disease grade for WT mice used for tissue analysis at the time of tissue harvesting was 2.08 ± 0.86 , whereas average score for Wld^s mice used was 1.33 ± 0.75 ($P = \text{NS}$, Student's *t*-test). Axonal loss in Wld^s mice was limited to the lumbar spinal cord but was present at all levels in WT mice at much higher levels. **e:** Quantification of demyelination was performed using Luxol fast blue-stained sections and showed less demyelination at all levels of the spinal cord in Wld^s mice. **f:** Demonstration of quantification method used to calculate axonal loss. Transverse sections from the posterior column (P) of the lumbar spinal cord (L) from both WT and Wld^s mice were stained with the Bielschowsky method. The NIH Image analyzer program was used to calculate areas. The area with more than 50% axonal loss (outlined in green) is divided by the total white matter area of the posterior column (outlined in red), thus quantifying percent axonal loss, which is represented in **d** and **e**. There is more axonal loss in the WT sample than the Wld^s sample shown. **g:** Demonstration of method used to quantify demyelination. Transverse sections of the posterior column (P) and lumbar spinal cord (L) are stained with Luxol fast blue. Areas with demyelination (absence of Luxol fast blue stain) (outlined in green) are divided by the total white matter area of the posterior column (outlined in red), thus measuring percent demyelination represented in **e** and **g**. There is more demyelination in the WT sample than the Wld^s sample. Original magnifications: $\times 400$ (**b**); $\times 5000$ (**c**).

significantly less in Wld^s samples ($4.96 \pm 1.85\%$), compared with WT samples ($28.82 \pm 2.96\%$, $P < 0.0001$; Student's *t*-test). In addition, total demyelination was diminished in Wld^s mice ($3.37 \pm 1.25\%$) compared with WT mice ($22.23 \pm 4.84\%$, $P = 0.003$; Student's *t*-test). The methods used to calculate axonal loss and demyelination are outlined in Figure 1, f and g.

Preserved Peripheral Immune Responses to Myelin Antigen in Wld^s

We examined T-cell proliferation, proinflammatory (Th1) and Th2 cytokine production by *in vivo* primed splenocytes to immunizing antigen (MOGp35-55) from WT and Wld^s mice. T cells from both groups proliferated equally well, indicating

Table 1. Composite of Five Experiments Followed for 60 Days

No. of mice	Mean day onset	Mean maximal grade			No. of deaths	Area under curve
		Day 0 to 20	Day 20 to 40	Day 40 to 60		
WT	16	10.88 ± 1.45	2.34 ± 0.72	2.16 ± 0.47	2.12 ± 0.93	0
Wld ^s	28	17.58 ± 9.3	0.98 ± 1.19	1.56 ± 1.21	1.67 ± 0.31	0
P value		0.0068	0.0002	0.064	0.3405	0.0017

Mean day of onset ± SD, and mean maximal grade ± SD are shown. Analysis was performed using Mann-Whitney U-test. P values < 0.05 were considered significant.

that there was no defect in priming (Figure 2a). Production of IFN- γ , a Th1 cytokine, as well as the Th2 cytokines IL-10 and IL-5, was similar in supernatants of primed splenocytes from WT and Wld^s mice (IFN- γ , IL-10, and IL-5, P = NS) (Figure 2, b-d). There was no difference in IL-6 production as assessed by ELISA (not shown). Furthermore, delayed-type hypersensitivity response, which reflects the competence of the peripheral immune response to immunizing antigen, was similar in WT and Wld^s mice (P = NS) (Figure 2e). These studies indicate that T cells from Wld^s mice are primed by myelin antigen and suggest that the observed phenotype of attenuated clinical disease is not related to differences in the peripheral immune response between Wld^s and WT mice.

Decreased Macrophage/Microglia Accumulation and Activation in the CNS of Wld^s Mice with EAE

Given the similarity in peripheral immune response in Wld^s and WT mice, we asked whether altered immune responses within the CNS may account for disease attenuation in Wld^s mice with EAE. We analyzed the migration of inflammatory cells into the CNS by staining spinal cord sections at various time points for CD4⁺ T-cell, CD8⁺ T-cell, and macrophage/microglia markers. We found that macrophage/microglia immunoreactivity was strikingly absent in the spinal cords of Wld^s mice at early time points after immunization (day 12) but present in WT mice (Figure 3a). Moreover, at subsequent time points, parenchymal infiltration of macrophages/microglia but not T cells was significantly less in Wld^s mice although periventricular infiltration of macrophages/microglia was present (Figure 3b). By flow cytometry, we analyzed immune cell populations present in the spinal cord of WT and Wld^s mice with EAE. Confirming our histology results, we found that both CD11b⁺CD45lo and CD11b⁺CD45hi cells, consistent with microglia and macrophages, respectively, were decreased in Wld^s mice (Figure 9, c and d).

Increased Expression of CD200 in the Spinal Cord of Wld^s Mice

Because our initial studies demonstrated a significant suppression of macrophage/microglia accumulation in the CNS of Wld^s mice with EAE, we investigated the expression of molecules that have been previously shown to modulate macrophage/microglial function.

CD200 is a nonsignaling molecule predominantly expressed on neurons,^{18–20} and studies in CD200-deficient mice suggest that ligation of the CD200R delivers a negative signal for microglia/macrophage activation.^{21–24}

We found that CD200 protein expression was elevated in spinal cord homogenates from naïve Wld^s mice (Figure 6a) and increased dramatically throughout the course of EAE, both in spinal cord homogenates (Figure 6a) and by immunofluorescence staining of spinal cord (Figure 4a). Using confocal microscopy of the spinal cord, we found markedly enhanced expression of CD200 in naïve Wld^s mice, compared with WT mice, co-localizing with the neuronal marker NeuN (Figure 4, b–e). Staining for CD200 was located on both the surface and cytoplasm of neurons and their axons (Figure 4, c–f). In addition, we found a modest increase in CD200 expression on oligodendrocytes (Figure 5a) and astrocytes (Figure 5b) after immunization in both strains. We found no significant difference in expression of CD200 on T-cell, B-cell, or macrophage populations between WT and Wld^s mice (Table 2).

Toll-like receptors (TLRs) regulate innate immune responses and are widely expressed on microglia as well as astrocytes. We found no difference in expression of TLR-2, -4, or -9 in the CNS between naïve or immunized Wld^s or WT mice (TLR-4 shown in Figure 7c). Neuronal expression of CD22 has been shown to regulate microglial activation.³⁴ We did not find any difference in CD22 expression by immunoblot in spinal cord lysates of Wld^s and WT mice (Figure 7c). Fractalkine (CX3CL1) has recently been shown to play a regulatory role in CNS inflammation.³⁵ We found no significant differences in fractalkine expression in spinal cord homogenates between Wld^s and WT mice (Figure 7d).

Previously reported functions of the Wld^s gene include altered synaptic transmission,⁴ resistance to calpain-induced proteolysis,^{36,37} and vincristine- and paclitaxel-induced neuropathy,^{7,8} altered glutamate metabolism,³⁸ as well as altered immune responses to axon injury,¹³ suggesting that one or more molecules are affected by the Wld^s gene. Thus, we screened for differential expression of a number of molecules using immunofluorescence staining and Western blot analysis in WT and Wld^s mice related to these functions, including calpain I and II, synaptophysin, synaptogogmin, SNAP-25, Nogo, GAP-43, p-CREB, and nuclear factor- κ B, but we found no significant differences between Wld^s and WT mice (data not shown).

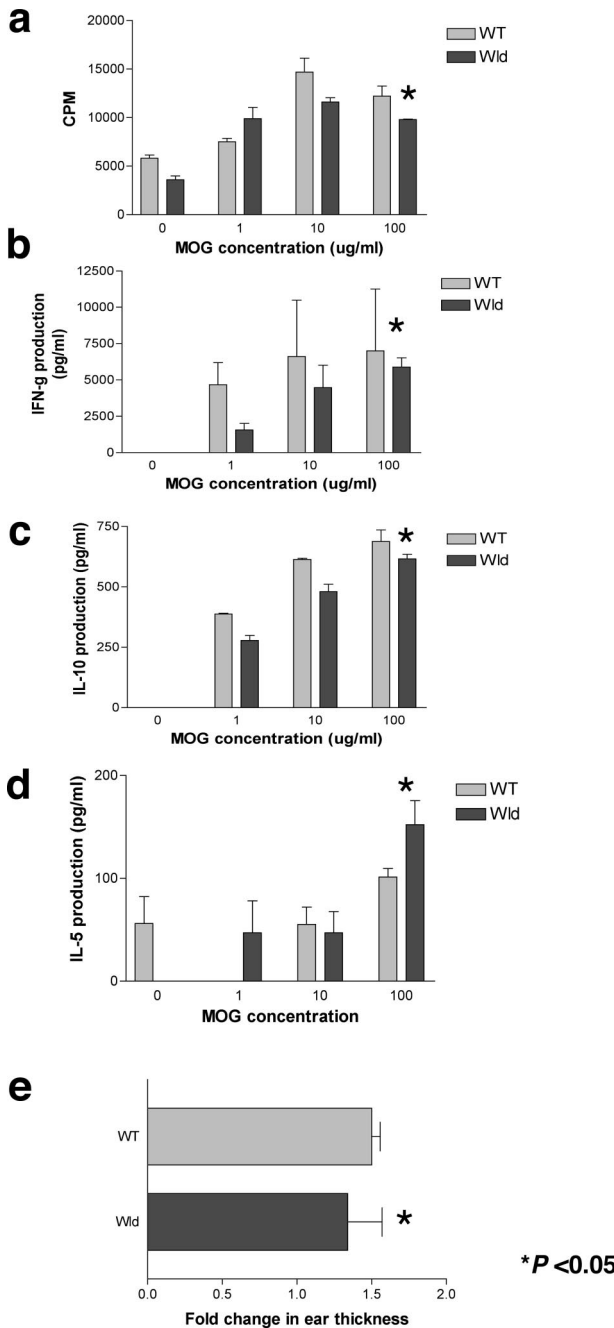


Figure 2. Immune responses to immunizing antigen are similar in *Wld*^s and WT mice. **a-d:** Splenocytes were harvested from *Wld*^s and WT mice 14 days after immunization with MOGp35-55 and then restimulated *in vitro* with MOGp35-55. **a:** Proliferative responses to immunizing peptide were similar in WT and *Wld*^s mice ($P = \text{NS}$, Student's *t*-test). **b:** IFN- γ production after restimulation with MOGp35-55 was similar in WT and *Wld*^s mice ($P = \text{NS}$, Student's *t*-test). **c:** IL-10 production was similar in both groups ($P = \text{NS}$, Student's *t*-test). **d:** IL-5 production was similar in both groups ($P = \text{NS}$, Student's *t*-test). **e:** Delayed-type hypersensitivity responses to MOGp35-55 in immunized mice were similar in WT and *Wld*^s mice ($P = \text{NS}$, Student's *t*-test). Results from four to six mice per group were averaged.

Decreased Ubiquitination of CD200 in the Spinal Cord of *Wld*^s Mice

The *Wld*^s gene is a triplication composed of the N-terminal region of *Ube4b* as well as the *Nmnat* gene.⁸ *Ube4b* is a

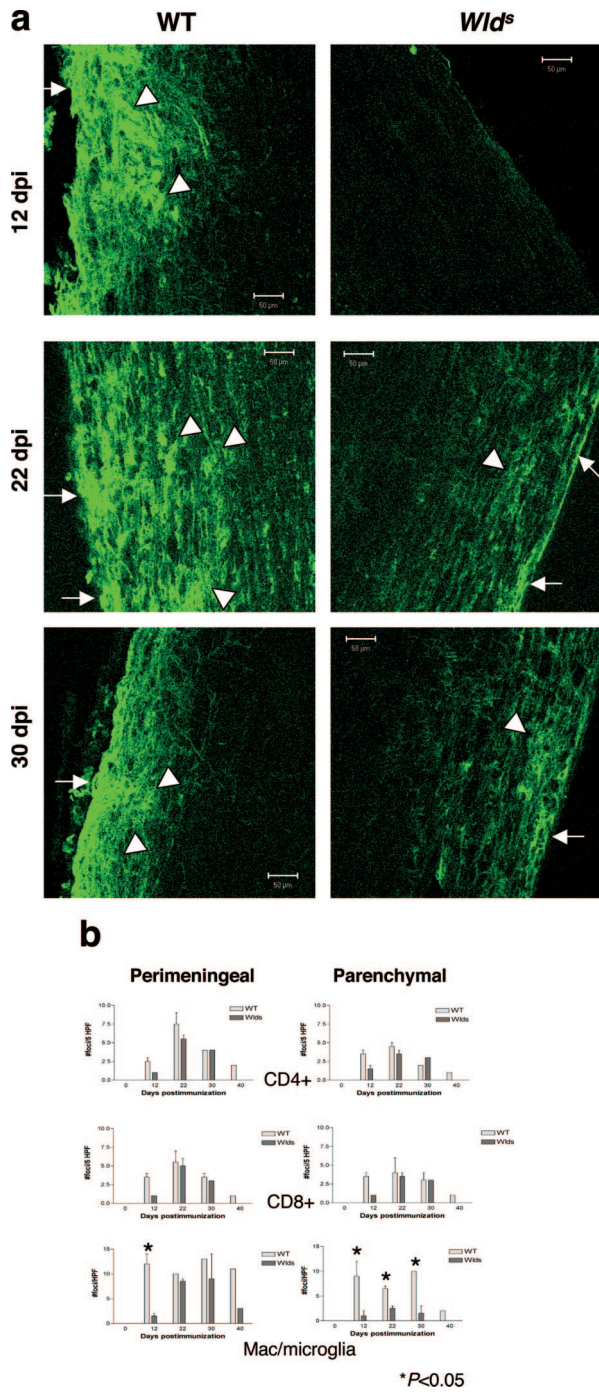


Figure 3. Reduced accumulation and activation of macrophages/microglia in the CNS in *Wld*^s mice during EAE. **a:** Representative photomicrographs of spinal cord sections taken from WT and *Wld*^s mice at days 12, 22, and 30 after immunization with MOGp35-55 and stained for Lectin-B4. Sections from WT mice show both perimeningeal/perivascular (arrowheads) and parenchymal infiltrates (white arrows) of cells from days 12 to 30. In contrast, sections from *Wld*^s mice lack macrophage/microglia infiltrates at day 12 and have fewer parenchymal infiltrates at other time points. **b:** Quantification of perimeningeal and parenchymal infiltrates of CD4 T cells, CD8 T cells, and macrophage/microglia from *Wld*^s and WT mice during the course of EAE showed that perimeningeal ($P < 0.05$) and parenchymal infiltrates ($P < 0.05$) of macrophages/microglia were significantly less in *Wld*^s mice at day 12 after immunization. In addition, at later time points, parenchymal infiltration (d22, $P < 0.05$; d30, $P < 0.05$) of macrophages/microglia in sections from *Wld*^s mice was significantly reduced compared with WT mice. In contrast, perimeningeal and parenchymal infiltrates of CD4 and CD8 cells were similar in both groups at all time points. Statistical analysis was performed using unpaired Student's *t*-test. Original magnifications, $\times 20$.

member of the E4 family, which regulates multiubiquitination of proteins targeted for degradation by the 26S proteasome complex.³⁹ We hypothesized that the *Wld^s* gene may be responsible for alterations in ubiquitination of CD200, potentially leading to decreased degradation and increased expression of CD200. To assess this, we studied the ubiquitination of CD200 immunoprecipitated from spinal cord lysates from both groups. Immunoprecipitates were immunoblotted with either ubiquitin or CD200 (Figure 6c). Ubiquitination of CD200 was significantly decreased in *Wld^s* immunoprecipitates of CD200 at day 0 and day 22 after immunization. This finding is even more striking given the relatively higher amounts of CD200 immunoprecipitated from *Wld^s* compared with WT spinal cords. At day 60 after immunization, the relative expression of ubiquitin in *Wld^s* CD200 lysates increased, suggesting a temporal relationship between ubiquitination of this substrate.

CD200R Is Expressed on Splenocytes and CNS Glial Cells

Because CD200 is a nonsignaling molecule, we examined the expression of CD200 receptor (CD200R) on splenocytes as well as populations of CNS cells to explore the potential effectors of CD200R ligation. Using flow cytometry, we found that CD200R is expressed at similar levels on some CD11b⁺ and CD11c⁺ cells in naïve and activated splenocytes from both WT and *Wld^s* mice (Figure 7, a and b). We found similar quantities of CD200R in spinal cord lysates from naïve and EAE mice in both strains (Figure 7c). Using confocal microscopy we found that in the spinal cord, CD200R is expressed on microglia and macrophages (LB4⁺ cells) (Figure 8). By flow cytometry, we found that between 40 to 45% of microglia from the BV-2 cell line expressed CD200R (data not shown). We studied the expression of CD200R in the CNS using an anti-CD200R antibody directed against peptide 313015, which is present in CD200R isoforms R1, -2, and -4, described in Gorczynski and colleagues.²⁶ We found that CD200R was expressed on astrocytes (GFAP⁺ cells) and oligodendrocytes (CNPase⁺ cells) but not on neurons or axons (β -tubulin⁺ processes) (Figure 8). These results were confirmed with studies using a second antibody directed against CD200R (clone OX-110)²³ (data not shown).

*Protection from EAE in *Wld^s* Model Is Associated with Decreased CNS Expression of IL-6*

To explore potential mechanisms of CD200-CD200R-mediated protection, we examined cytokine expression in the CNS of *Wld^s* and WT mice. We found that IL-6 levels were decreased in spinal cord lysates from *Wld^s* mice with EAE compared with WT mice ($P < 0.05$) (Figure 7c). Moreover, IL-10 was significantly elevated in *Wld^s* spinal cords after the induction of EAE ($P < 0.02$) (Figure 7c). However, there was no significant difference in tumor

necrosis factor- α expression at either time point. Immunofluorescent staining showed no difference in inducible nitric-oxide synthase expression in the CNS between the two strains (data not shown).

*Administration of a Blocking Anti-CD200 Antibody Abrogates in Vivo Protection in *Wld^s* Mice*

To confirm that overexpression of CD200 is responsible for disease attenuation in the *Wld^s* EAE model, we administered an anti-CD200 blocking antibody to both WT and *Wld^s* mice during the effector stage of disease (Figure 9a). To investigate the immunomodulatory effects of the CD200-CD200R pathway within the CNS, rather than its potential effects on peripheral T-cell priming, we began treatment after the onset of disease (day 10 to 20) after T cells had already been fully primed and inflammatory cells had entered the CNS. We found that administration of anti-CD200 antibody worsened disease in *Wld^s* mice, whereas there was little effect in WT mice. Moreover, infiltration of macrophages and microglia into the parenchyma of *Wld^s* spinal cords was enhanced after treatment with anti-CD200 antibody (Figure 9, b-d). Axonal damage as reflected by staining for nonphosphorylated neurofilament (SMI-32)-positive axonal ovoids, was also increased in anti-CD200 antibody-treated *Wld^s* mice (Figure 9b).

*Increased Expression of CD200 in *Wld^s* Neuronal Cultures Is Associated with Neuroprotection from Microglia-LPS-Induced Toxicity*

To confirm that overexpression of CD200 *Wld^s* neurons is neuroprotective in the setting of inflammation-induced damage, we used an *in vitro* model of microglia-mediated neurotoxicity.⁴⁰ Neuronal cultures were prepared from E16-18 WT and *Wld^s* embryos and exposed to activated primary microglia. Expression of CD200 was higher in *Wld^s* compared with WT neuronal cultures, consistent with our *in vivo* observations (Figure 10a). The addition of LPS-activated (Figure 10b) or IFN- γ -activated (Figure 10c) primary microglia resulted in neuronal cell body destruction, with greater than 70% axonal beading in WT neuronal cultures, whereas *Wld^s* neurons and axons remained intact. Furthermore, the addition of anti-CD200 antibody or anti-CD200F(Ab')₂ abrogated the protection seen in *Wld^s* co-cultures but did not exacerbate neuronal loss in WT co-cultures (Figure 10, b and c).

Discussion

Our results demonstrate that the CD200-CD200R pathway plays an important role in axonal protection in the setting of inflammation-mediated neurodegeneration. We found that *Wld^s* mice experience an attenuated EAE disease course, which was mediated by selective elevation

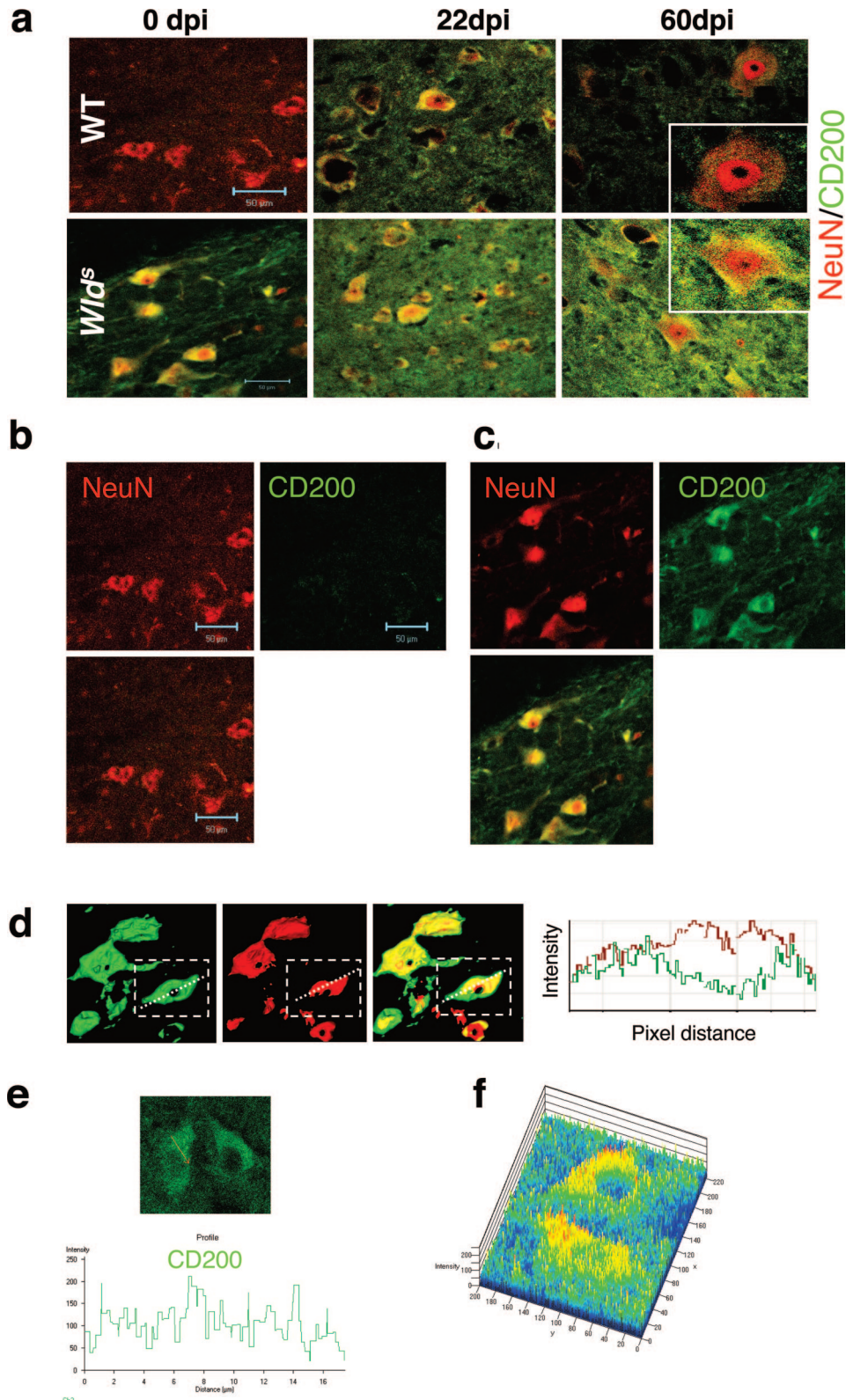


Figure 4. Increased expression of CD200 in the spinal cord of *Wld^s* mice. Spinal cord sections from WT and *Wld^s* mice on days 0, 22, and 60 after immunization were double-stained with CD200 (green) and NeuN (red) marker for neurons. **a:** Shown are representative merged confocal images. CD200 expression is markedly increased in *Wld^s* sections compared with WT sections, with increasing expression after the induction of EAE. **b** and **c:** Split confocal images showing co-localization of CD200 and NeuN staining in WT (**b**) and *Wld^s* (**c**) sections. CD200 expression is increased on *Wld^s* neuronal bodies and processes. **d:** Confocal merge profiles and intensity profile shows co-localization of CD200 (green) and NeuN (red) in the surface and cytoplasm of cells and processes but not the nucleus. **e:** Confocal intensity profile of CD200 staining shows a punctate pattern of staining consistent with surface staining of the molecule. **f:** Confocal reconstruction (2.5-dimension) of Z-stacked images demonstrates punctate areas of high-intensity staining (red > yellow > green), consistent with surface staining (red), as well as medium intensity staining in cytoplasmic regions (yellow). Original magnifications, $\times 63$.

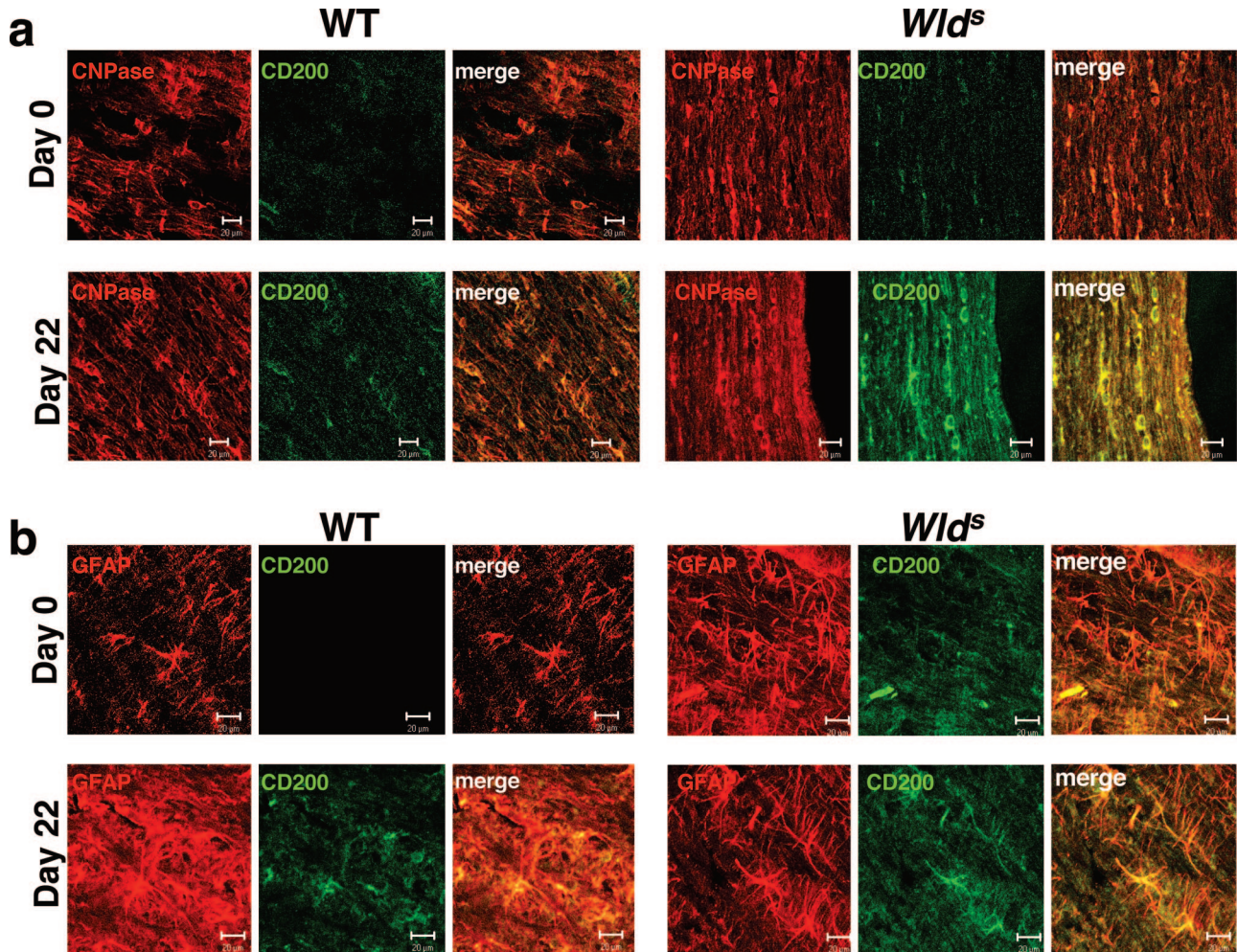


Figure 5. Increased expression of CD200 during EAE co-localizes with CNPase and GFAP marker. **a:** Splitway confocal images show partial co-localization of CD200 and CNPase markers in *Wld^s* and WT spinal cord sections. Expression in both strains is enhanced at day 22 after immunization compared with naïve spinal cords. **b:** Splitway confocal images show partial co-localization of CD200 and GFAP markers in *Wld^s* and WT spinal cord sections. Expression is enhanced particularly in *Wld^s* sections at day 22 after immunization compared with naïve spinal cords. Original magnifications, $\times 63$.

of the CD200 molecule primarily on CNS neurons and partially on glial cells. Elevated expression of CD200 resulted in diminished accumulation of macrophages and microglia in the CNS with reduced IL-6 and enhanced IL-10 expression in the CNS and suppression of secondary immune-mediated axonal damage and demyelination in the EAE model. In addition, we demonstrate that enhanced expression of CD200 protected neurons from microglial-mediated damage *in vitro*. CD200 and its receptor were similarly expressed in the peripheral immune system of *Wld^s* and WT mice, indicating that our observations are CNS-specific. Moreover, CD200R was similarly expressed in the CNS of *Wld^s* and control mice, indicating that our findings are dependent on altered expression of CD200 but not its receptor. Interestingly, we found that the CD200 receptor is expressed on astrocytes and oligodendrocytes as well as on microglia and macrophages, suggesting that CD200-CD200R interactions can play multiple roles in the regulation of CNS events. Elevated expression of CD200 was associated with defective ubiquitination of the protein in the *Wld^s* CNS, indicating involvement of the ubiquitin-proteasome

pathway and potentially the *Ube4b* portion of the *Wld^s* gene.

CD200 belongs to the immunoglobulin superfamily of glycoproteins and has been previously shown to be expressed on some populations of neurons.^{18–20} The CD200 receptor has been previously demonstrated on macrophages and microglia^{21–23} and more recently has been shown to be expressed on mast cells, basophils, dendritic cells, and polarized Th2 cells.^{23,28} CD200 is a nonsignaling molecule, whereas CD200R activation initiates tyrosine phosphorylation.²¹ Macrophage and microglial responses to nerve trauma and EAE were found to be accelerated in mice deficient for CD200,²⁴ the converse of our findings in *Wld^s* mice. Worsening of EAE in CD200-deficient mice was associated with enhanced macrophage infiltrates and expression of inducible nitric-oxide synthase in the CNS. In the *Wld^s* model, we did not observe alterations in inducible nitric-oxide synthase or nitrate levels, but we did find that protection from EAE was associated with decreased IL-6 levels in the CNS. IL-6 is a proinflammatory cytokine and is predominantly synthesized by mononuclear phagocytes. Transgenic ex-

Table 2. Expression of CD200 in Splenocytes from *Wld^s* Mice

	Naive		Day 12 after immunization	
	WT	<i>Wld^s</i>	WT	<i>Wld^s</i>
%CD3 ⁺	48.39	39.93	28.74	26.79
%CD3 ⁺ /CD200 ⁺	0.17	0.38	0.36	0.54
%CD4 ⁺	31.93	33.85	25.06	23.21
%CD4 ⁺ /CD200 ⁺	0.14	0.14	1.75	2.02
%CD8 ⁺	6.61	7.65	12.1	8.73
%CD8 ⁺ /CD200 ⁺	0.17	0.04	0	0
%CD11b ⁺	8.22	11.69	11.48	11.97
%CD11b ⁺ /CD200	0.13	0.28	0.47	0.5
%CD19 ⁺	34.77	29.66	55.4	51.72
%CD19 ⁺ /CD200 ⁺	0.08	0.14	0.27	0.09
Total number of cells/ spleen × 10 ⁶	52	67.3	104	152

Flow cytometric analysis of splenocytes, quantifying T-cell, B-cell, or macrophage populations and CD200 expression on each cell type from WT and *Wld^s* mice was performed. Splenocytes from naïve mice and mice immunized with MOGp35–55 (day 12 after immunization) were assessed. Expression of CD200 on T-cell, B-cell, or macrophage populations was similar between the two strains at both time points. Expression of CD200 increased slightly on splenic CD4⁺ cells from both WT and *Wld^s* mice after immunization.

expression of IL-6 in the CNS resulted in enhanced astrocytosis and neurodegeneration.⁴¹ We also found increased expression of IL-10 in the CNS of *Wld^s* mice with EAE. IL-10 has been shown to down-regulate immune responses in EAE⁴² and may play a role in neuroprotection.⁴³

Our studies in the *Wld^s* model were motivated by the goal of identifying molecules involved in axonal protection. Previously reported functions of the *Wld^s* gene include altered synaptic transmission,⁴ resistance to calpain-induced proteolysis,^{36,37} and vincristine- and paclitaxel-induced neuropathy,^{7,8} altered glutamate metabolism,³⁸ as well as altered immune response to axon injury,¹³ suggesting that one or more molecules are affected by the *Wld^s* gene. In addition to examining expression of CD200, we screened for a number of molecules related to these functions, including calpain, synaptic proteins, and proteins involved in neurite growth, as well as expression of nuclear factor- κ B, with negative results. Recent work has suggested that *in vitro* axonal protection is associated with the function of the *Nmnat* portion of the *Wld^s* gene through altered NAD-dependent processes in the nucleus⁴⁴ or in the degenerating axons.⁴⁵ Transfection of the *Wld^s* gene or *Nmnat-1* gene, or administration of NAD⁴⁴ or nicotinamide,⁴⁵ reduces Wallerian degeneration and is protective in EAE.¹⁵ However, in both the Araki and colleagues⁴⁴ and Wang and colleagues⁴⁵ studies, it was noted that the neurons transfected with *Nmnat-1* did not survive as long as neurons transfected with the *Wld^s* gene, indicating that *Nmnat* expression alone only partially explains the *Wld^s* phenotype.

Consistent with the observation that *Nmnat-1* only partially explains the *Wld^s* phenotype, we found that ubiquitination of CD200 was impaired in the *Wld^s* model, suggesting that the ubiquitin-proteasome pathway through the *Ube4b* moiety of the *Wld^s* gene plays a pri-

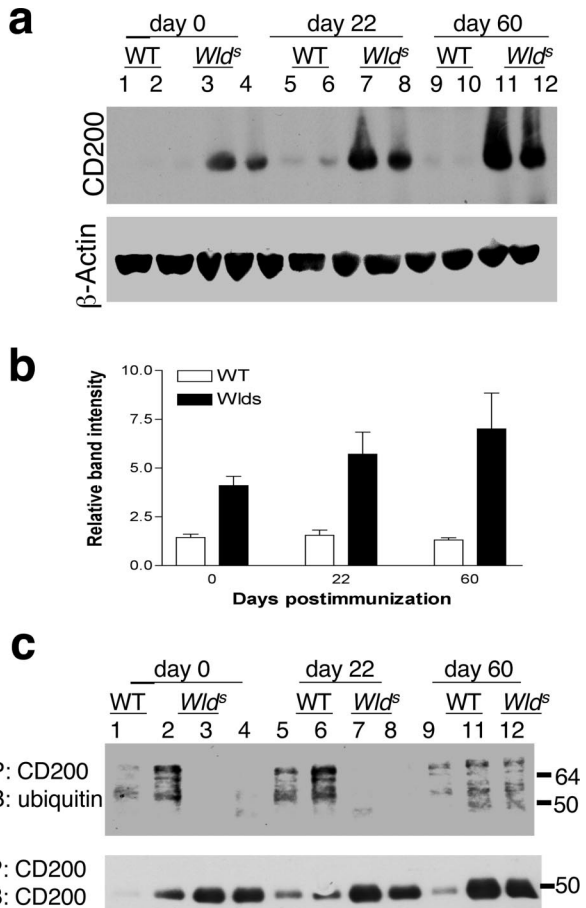


Figure 6. Decreased ubiquitination of CD200 in spinal cord lysates of *Wld^s* mice. **a:** Representative immunoblot of spinal cord lysates from naïve WT mice (**lanes 1** and **2**), naïve *Wld^s* mice (**lanes 3** and **4**), WT mice day 22 after immunization (**lanes 5** and **6**), *Wld^s* mice day 22 after immunization (**lanes 7** and **8**), WT mice day 60 after immunization (**lanes 9** and **10**), and *Wld^s* mice day 60 after immunization (**lanes 11** and **12**) shows increased expression of CD200 in *Wld^s* spinal cord lysates at all time points compared with those from WT mice. β -Actin control immunoblot shows similar protein amounts in all samples. **b:** Densitometric quantification of immunoblots demonstrates increased expression of CD200 during the course of EAE in *Wld^s* mice but not WT mice. **c:** Immunoprecipitation of CD200, with immunoblotting (IB) of ubiquitin and CD200. Sample numbers are the same as in **a**, except sample 10 was omitted. There was decreased expression ubiquitination of CD200 in *Wld^s* mice samples at d0 and d22 compared with WT samples. At d60, the expression of ubiquitin was increased in *Wld^s* samples and was comparable with the WT sample.

mary role in regulating the expression of neuroprotective molecules, including CD200. The yeast homologue of *Ube4b*, *UFD2*, has been shown to be involved in tolerance to stress through the degradation of stress-induced aberrant proteins.³⁹ *In vitro* and *in vivo*, inhibition of the ubiquitin-proteasome pathway profoundly delayed axonal degradation after transection,⁴⁶ bearing a striking resemblance to the *Wld^s* phenotype. Moreover, mutations in ubiquitin-proteasome pathway-related enzymes are responsible for several neurodegenerative diseases, including autosomal recessive juvenile Parkinson's disease⁴⁷ and the gracile axonal dystrophy mouse model.⁴⁸ Our finding that CD200 expression is dependent on ubiquitination suggests that the *Ube4b* portion of the *Wld^s* gene regulates the expression of CD200 and, possibly, additional molecular targets. A wide array of phenotypes

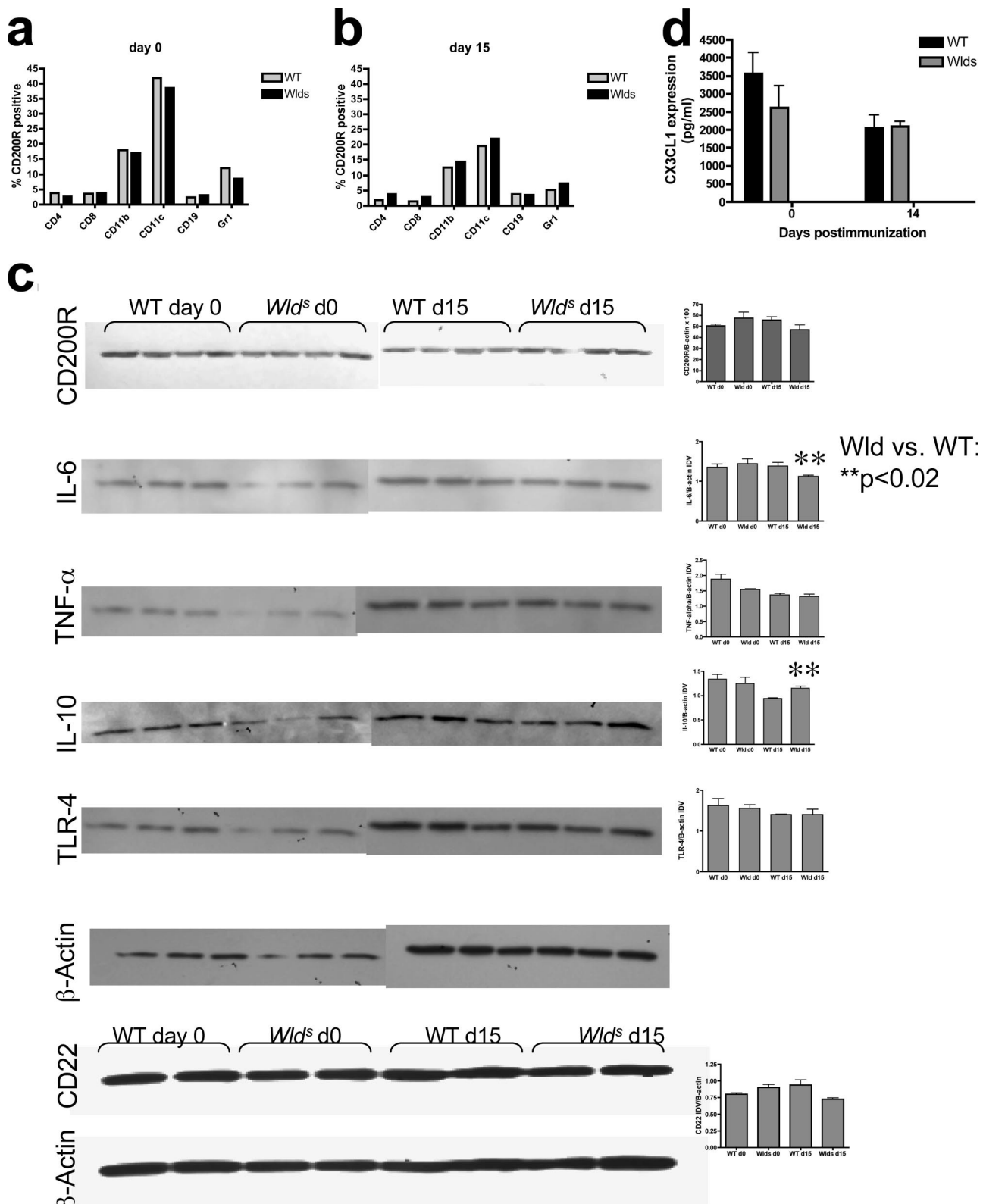


Figure 7. CD200R expression in *Wld^s* and WT splenocytes and CNS. CD200R expression was assessed by flow cytometry in WT and *Wld^s* splenocyte populations on day 0 (**a**) and at day 15 (**b**) after immunization. CD200R was predominantly found on naïve CD11b⁺ and CD11c⁺ cells in both strains with no significant difference between the WT and *Wld^s* strains. Expression of CD200R decreased after immunization on these cells. **c:** Protein levels were assessed in spinal cord lysates from WT and *Wld^s* mice on day 0 and day 15 after immunization, by Western blot, and expressed as protein/β-actin IDV values. There was no significant difference in CD200R expression between the strains. IL-6 was reduced and IL-10 was elevated in *Wld^s* mice compared with WT mice after immunization at day 15 after immunization. There was no significant difference in tumor necrosis factor-α, TLR-4, or CD22 expression between the two strains at either time point. **d:** Fractalkine (CX3CL1) concentration in spinal cord homogenates from WT and *Wld^s* at day 0 and day 14 after immunization was assessed using ELISA assay. Results from four mice/group/time point were averaged. There was no significant difference between WT and *Wld^s* mice at either time point.

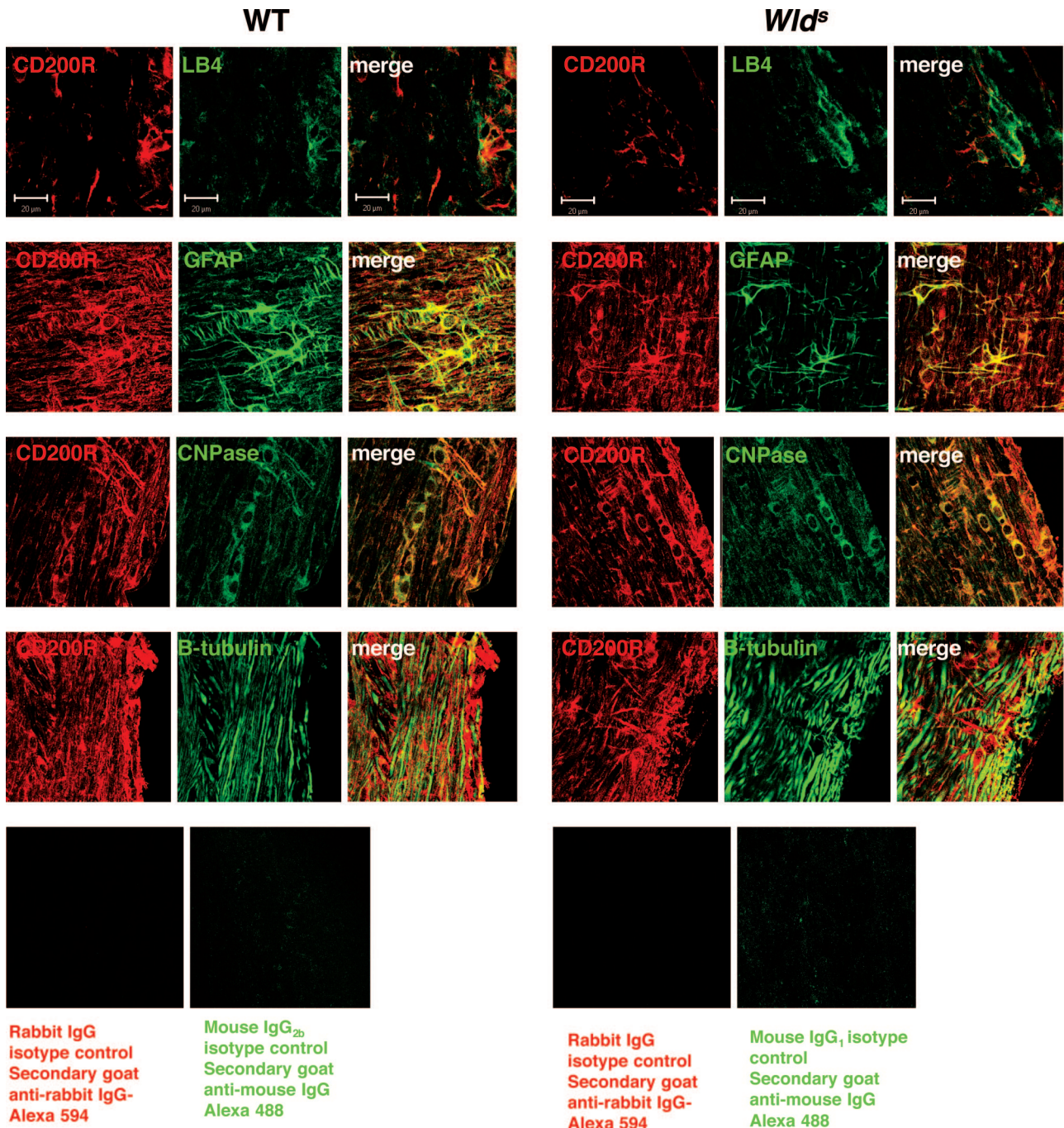


Figure 8. CD200R is expressed on microglia, oligodendrocytes, and astrocytes. Spinal cord sections from WT and *Wld^s* mice on days 0, 22, and 60 after immunization were double-stained with CD200R (red) and LB4-microglial or GFAP (astrocytes) or CNPase (oligodendrocytes) or β -tubulin (axons and neurons). Shown are representative merged confocal images from mice on day 22 after immunization. CD200R staining was present on microglia/macrophages as well as astrocytes and oligodendrocytes from both strains. CD200R was not present on axons/neurons. Original magnifications, $\times 63$.

have now been ascribed to the *Wld^s* gene, and it is possible that in addition to CD200, the *Wld^s* chimeric protein specifically alters E4 system-mediated multiubiquitination of multiple substrates, leading to diminished degradation by the 26S proteasome complex. Moreover, NAD levels may also alter gene expression of additional targets. In support of the concept that the *Wld^s* gene affects the expression of more than one molecule, Gillingswater and colleagues⁴⁹ recently performed a mRNA

screen of *Wld^s* and WT CNS tissue and demonstrated differential gene expression of several genes. In this study, however, a target neuroprotective pathway was not identified, in contrast to our results identifying elevated expression of CD200 as a critical neuroprotective molecule.

The *Wld^s* gene has classically been associated with delayed Wallerian degeneration after axon transection. Several studies have also demonstrated delayed macro-

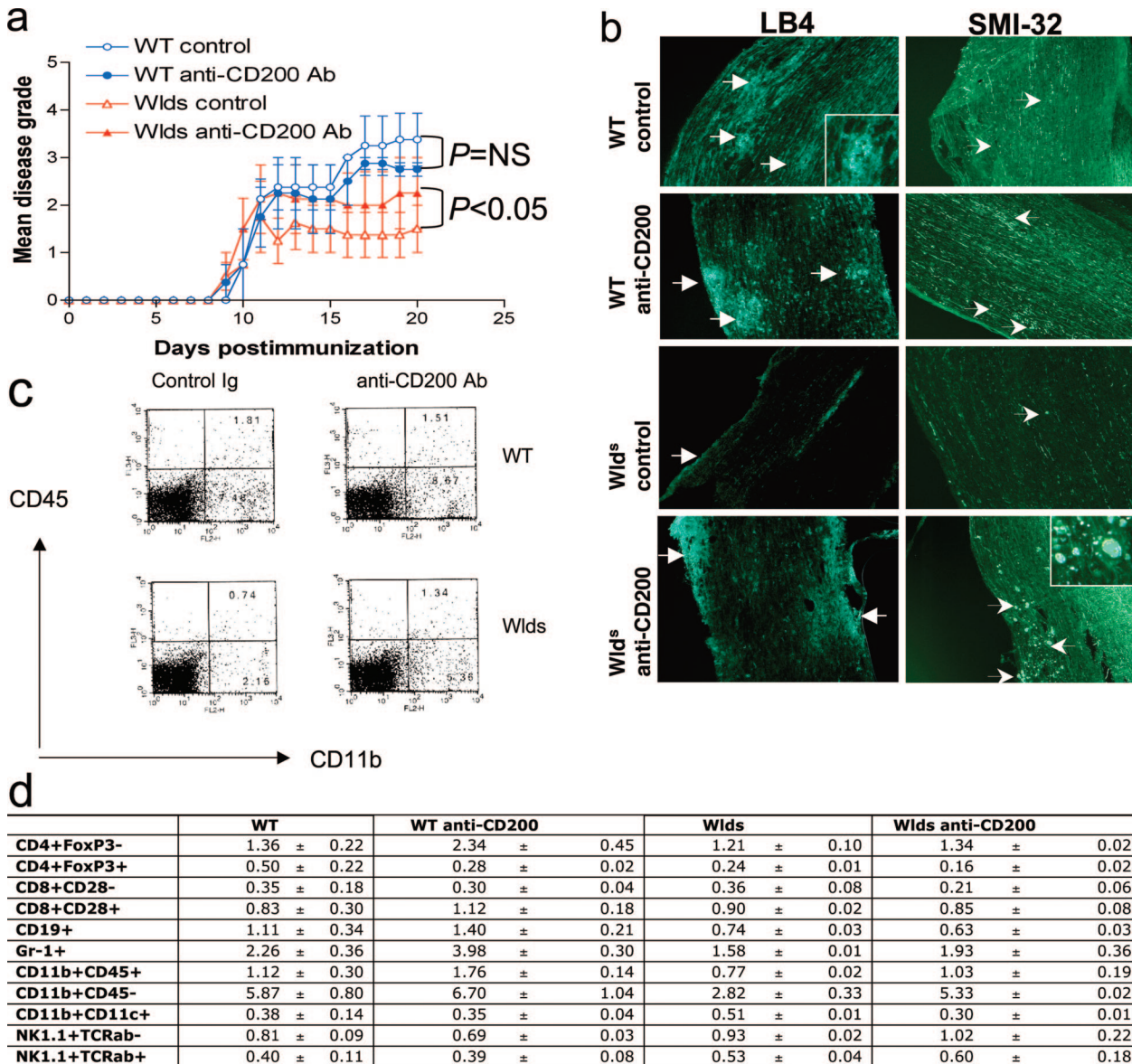


Figure 9. Treatment of *Wld^s* mice with blocking anti-CD200 antibody results in worsened EAE with increased macrophage/microglia infiltrates in the CNS. After the induction of EAE, *Wld^s* and WT mice were treated with 200 µg/100 µl of blocking anti-CD200 antibody injected intraperitoneally every other day from days 10 to 20. Control WT and *Wld^s* mice were treated with PBS alone. Eight mice per treatment group were evaluated. **a:** *Wld^s* mice treated with anti-CD200 antibody experienced a more severe disease course than untreated *Wld^s* mice ($P < 0.05$, Student's *t*-test—area under the curve). In comparison, disease in WT mice was similar even after treatment with anti-CD200 antibody ($P = \text{NS}$, Student's *t*-test). **b:** Spinal cord sections harvested at day 20 from treated and control mice demonstrate enhanced immunofluorescence staining of macrophages/microglia (white arrows) in the CNS of anti-CD200-treated *Wld^s* mice compared with *Wld^s* controls. Macrophage/microglia staining was similar in treated and untreated WT mice. Immunofluorescence staining demonstrates more SMI-32-positive axonal ovoids (white arrows) in the spinal cord white matter of treated *Wld^s* mice, compared with untreated controls. **c** and **d:** We performed flow cytometric analysis of immune cell populations in the spinal cords isolated from WT and *Wld^s* mice treated with anti-CD200 antibody or rat IgG control antibody (days 10 to 20) on day 20 after immunization. The results from three to four mice per group were averaged and are shown in table form in **d**. Also shown is a representative FACS analysis of spinal cords from WT and *Wld^s* mice treated with control Ig or anti-CD200 antibody and stained with CD11b-phycerythrin and CD45-allophycocyanine (APC) antibodies (**c**). Original magnifications, $\times 10$.

phage or microglial activation in the vicinity of the transected nerve, but its significance as a cause or consequence of delayed Wallerian degeneration has been unclear. In contrast to models of axon-transection or toxicity, suppression of local macrophage or microglial activation plays a critical role in diseases such as MS, in which neurodegeneration is primarily caused by inflammation. Thus, our results support previous observations showing decreased macrophage/microglial activation in transected nerves of *Wld^s* mice; however, in contrast to

classical axonal transection models, we show that in the EAE model, this mechanism plays a pivotal role in neuroprotection and is mediated by elevated expression of CD200.

Our findings highlight the importance of distinguishing the two phases of neurodegeneration in MS and its models.^{50–53} The first phase is a direct consequence of inflammation and includes cell, cytokine, complement, and antibody-mediated toxicity, which affects both axons and myelin. Axonal damage in MS lesions

has been shown to correlate strongly with the presence of activated macrophages/microglia as well as CD8⁺ T cells.¹⁶ Progressive forms of MS are associated with diffuse axonal damage and microglial activation.¹⁷ Strategies to enhance CNS expression of molecules

that down-regulate microglia, such as CD200, may be therapeutically important during this phase. Other molecules such as fractalkine may modulate other arms of the CNS inflammatory response.³³ The second phase of axonal damage results from secondary damage within the axon, mediated primarily by glutamate and calcium-dependent proteases,^{54–57} and may cause irreversible and/or propagated damage to the axon, resembling Wallerian degeneration.^{58–60} Here, neuroprotective strategies targeting pathways intrinsic to the axon and neuron are needed. Progressive axonal and neuronal degradation may further incite CNS inflammatory responses, thereby potentiating a vicious cycle that results in chronic progressive damage in the CNS. Thus, as our data has demonstrated, strategies to regulate CNS inflammation, particularly microglial responses, are critical in preventing permanent neural damage and disease progression.

Our studies show that, in the EAE model, the *Wld^s* gene plays a critical role in the regulation of CNS inflammation and consequent demyelination and axonal damage through elevated expression of CD200. Strategies to enhance neuronal expression of CD200, or strategies that promote ligation of the CD200 receptor, may be a potent means of reducing CNS pathology in MS.

Acknowledgment

We thank Lauren Friedman for technical support.

References

- Trapp BD, Peterson J, Ransohoff RM, Rudick R, Mork S, Bo L: Axonal transection in the lesions of multiple sclerosis. *N Engl J Med* 1998; 338:278–285
- Brown A, McFarlin DE, Raine CS: Chronologic neuropathology of relapsing experimental allergic encephalomyelitis in the mouse. *Lab Invest* 1982; 46:171–185
- Lunn ER, Perry VH, Brown MC, Rosen H, Gordon S: Absence of Wallerian degeneration does not hinder regeneration in peripheral nerve. *Eur J Neurosci* 1989; 1:27–33
- Mack TG, Reiner M, Beirowski B, Mi W, Emanuelli M, Wagner D, Thomson D, Gillingwater T, Court F, Conforti L, Fernando FS, Tarlton A, Andressen C, Addicks K, Magni G, Ribchester RR, Perry VH, Coleman MP: Wallerian degeneration of injured axons and synapses

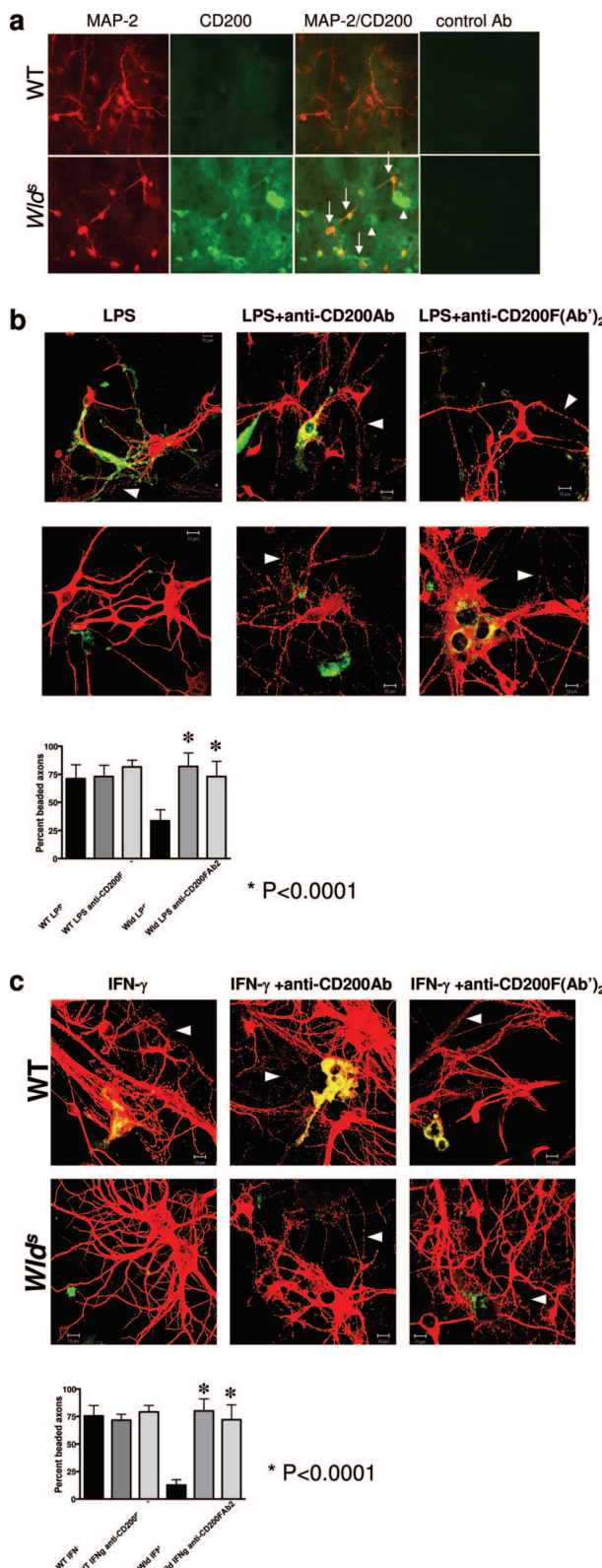


Figure 10. Neuronal cultures from *Wld^s* E16 embryos are protected from LPS-activated microglial-induced toxicity. Cortical neuronal cultures were derived from WT and *Wld^s* E16 embryos and plated at a high-density concentration of 200,000 cells/well/0.5 ml in 24-well plates. **a:** Representative fluorescence microscopy photomicrographs of MAP-2 (red), CD200 (green), and merged images from cortical cultures. CD200 expression is increased in *Wld^s* cultures compared with WT cultures, and co-localizes with MAP-2-positive cells (**white arrows**). In some cases, CD200 expression does not co-localize with MAP-2 (**arrowheads**). Controls are stained with isotype control antibody and secondary antibodies. **b** and **c:** Shown are representative photomicrographs of WT and *Wld^s* neuronal cultures with LPS-activated (**b**) or IFN-γ-activated (**c**) primary microglia. Cultures were immunostained with anti-MAP-2 antibody (red) and LB4 (green). *Wld^s* axons and neurons remain intact after co-culture with activated microglia; however, there is significant increase in axonal beading in WT co-cultures. Percentage of beaded axons/total number of axons in 10 fields was quantified for each condition. Protection of *Wld^s* neurons from neurotoxicity induced by activated microglia is ameliorated after the addition of a blocking anti-CD200 antibody or anti-CD200 F(AB')₂ fragment (both conditions, *P* < 0.0001; Student's *t*-test). Original magnifications, $\times 40$ (**a**) $\times 63$ (**b**, **c**).

- is delayed by a Ube4b/Nmnat chimeric gene. *Nat Neurosci* 2001, 4:1199–1206
5. Perry VH, Brown MC, Lunn ER: Very slow retrograde and Wallerian degeneration in the CNS of C57BL/Ola mice. *Eur J Neurosci* 1991, 3:102–105
 6. Deckwerth TL, Johnson Jr EM: Neurites can remain viable after destruction of the neuronal soma by programmed cell death (apoptosis). *Dev Biol* 1994, 165:63–72
 7. Wang MS, Davis AA, Culver DG, Glass JD: WldS mice are resistant to paclitaxel (taxol) neuropathy. *Ann Neurol* 2002, 52:442–447
 8. Wang MS, Fang G, Culver DG, Davis AA, Rich MM, Glass JD: The WldS protein protects against axonal degeneration: a model of gene therapy for peripheral neuropathy. *Ann Neurol* 2001, 50:773–779
 9. Steward O, Trimmer PA: Genetic influences on cellular reactions to CNS injury: the reactive response of astrocytes in denervated neuropil regions in mice carrying a mutation (Wld(S)) that causes delayed Wallerian degeneration. *J Comp Neurol* 1997, 380:70–81
 10. Schauwecker PE, Steward O: Genetic influences on cellular reactions to brain injury: activation of microglia in denervated neuropil in mice carrying a mutation (Wld(S)) that causes delayed Wallerian degeneration. *J Comp Neurol* 1997, 380:82–94
 11. Fujiki M, Zhang Z, Guth L, Steward O: Genetic influences on cellular reactions to spinal cord injury: activation of macrophages/microglia and astrocytes is delayed in mice carrying a mutation (Wld(S)) that causes delayed Wallerian degeneration. *J Comp Neurol* 1996, 371:469–484
 12. Lawson LJ, Frost L, Risbridger J, Fearn S, Perry VH: Quantification of the mononuclear phagocyte response to Wallerian degeneration of the optic nerve. *J Neurocytol* 1994, 23:729–744
 13. Shamash S, Reichert F, Rotshenker S: The cytokine network of Wallerian degeneration: tumor necrosis factor-alpha, interleukin-1alpha, and interleukin-1beta. *J Neurosci* 2002, 22:3052–3060
 14. Perry VH, Brown MC, Lunn ER, Tree P, Gordon S: Evidence that very slow Wallerian degeneration in C57BL/Ola mice is an intrinsic property of the peripheral nerve. *Eur J Neurosci* 1990, 2:802–808
 15. Kaneko S, Wang J, Kaneko M, Yiu G, Hurrell JM, Chitnis T, Khoury SJ, He Z: Protecting axonal degeneration by increasing nicotinamide adenine dinucleotide levels in experimental autoimmune encephalomyelitis models. *J Neurosci* 2006, 26:9794–9804
 16. Bitsch A, Schuchardt J, Bunkowski S, Kuhlmann T, Bruck W: Acute axonal injury in multiple sclerosis. Correlation with demyelination and inflammation. *Brain* 2000, 123:1174–1183
 17. Kutzelnigg A, Lucchinetti CF, Stadelmann C, Bruck W, Rauschka H, Bergmann M, Schmidbauer M, Parisi JE, Lassmann H: Cortical demyelination and diffuse white matter injury in multiple sclerosis. *Brain* 2005, 128:2705–2712
 18. Barclay AN, Brown MH: Heterogeneity of interactions mediated by membrane glycoproteins of lymphocytes. *Biochem Soc Trans* 1997, 25:224–228
 19. Clark MJ, Gagnon J, Williams AF, Barclay AN: MRC OX-2 antigen: a lymphoid/neuronal membrane glycoprotein with a structure like a single immunoglobulin light chain. *EMBO J* 1985, 4:113–118
 20. McCaughey GW, Clark MJ, Barclay AN: Characterization of the human homolog of the rat MRC OX-2 membrane glycoprotein. *Immunogenetics* 1987, 25:329–335
 21. Wright GJ, Puklavec MJ, Willis AC, Hoek RM, Sedgwick JD, Brown MH, Barclay AN: Lymphoid/neuronal cell surface OX2 glycoprotein recognizes a novel receptor on macrophages implicated in the control of their function. *Immunity* 2000, 13:233–242
 22. Preston S, Wright GJ, Starr K, Barclay AN, Brown MH: The leukocyte/neuron cell surface antigen OX2 binds to a ligand on macrophages. *Eur J Immunol* 1997, 27:1911–1918
 23. Wright GJ, Cherwinski H, Foster-Cuevas M, Brooke G, Puklavec MJ, Bigler M, Song Y, Jenmalm M, Gorman D, McClanahan T, Liu MR, Brown MH, Sedgwick JD, Phillips JH, Barclay AN: Characterization of the CD200 receptor family in mice and humans and their interactions with CD200. *J Immunol* 2003, 171:3034–3046
 24. Hoek RM, Ruuls SR, Murphy CA, Wright GJ, Goddard R, Zurawski SM, Blom B, Homola ME, Streit WJ, Brown MH, Barclay AN, Sedgwick JD: Down-regulation of the macrophage lineage through interaction with OX2 (CD200). *Science* 2000, 290:1768–1771
 25. Gorczynski RM: Transplant tolerance modifying antibody to CD200 receptor, but not CD200, alters cytokine production profile from stimulated macrophages. *Eur J Immunol* 2001, 31:2331–2337
 26. Gorczynski R, Chen Z, Kai Y, Lee L, Wong S, Marsden PA: CD200 is a ligand for all members of the CD200R family of immunoregulatory molecules. *J Immunol* 2004, 172:7744–7749
 27. Jenmalm MC, Cherwinski H, Bowman EP, Phillips JH, Sedgwick JD: Regulation of myeloid cell function through the CD200 receptor. *J Immunol* 2006, 176:191–199
 28. Zhang S, Cherwinski H, Sedgwick JD, Phillips JH: Molecular mechanisms of CD200 inhibition of mast cell activation. *J Immunol* 2004, 173:6786–6793
 29. Fallarino F, Asselin-Paturel C, Vacca C, Bianchi R, Gizzi S, Fioretti MC, Trinchieri G, Grohmann U, Puccetti P: Murine plasmacytoid dendritic cells initiate the immunosuppressive pathway of tryptophan catabolism in response to CD200 receptor engagement. *J Immunol* 2004, 173:3748–3754
 30. Gorczynski RM, Chen Z, Lee L, Yu K, Hu J: Anti-CD200R ameliorates collagen-induced arthritis in mice. *Clin Immunol* 2002, 104:256–264
 31. Gorczynski RM, Hu J, Chen Z, Kai Y, Lei J: A CD200FC immunoadhesin prolongs rat islet xenograft survival in mice. *Transplantation* 2002, 73:1948–1953
 32. Chitnis T, Najafian N, Benou C, Salama AD, Grusby MJ, Sayegh MH, Khoury SJ: Effect of targeted disruption of STAT4 and STAT6 on the induction of experimental autoimmune encephalomyelitis. *J Clin Invest* 2001, 108:739–747
 33. Huang D, Shi FD, Jung S, Pien GC, Wang J, Salazar-Mather TP, He TT, Weaver JT, Ljunggren HG, Biron CA, Littman DR, Ransohoff RM: The neuronal chemokine CX3CL1/fractalkine selectively recruits NK cells that modify experimental autoimmune encephalomyelitis within the central nervous system. *FASEB J* 2006, 20:896–905
 34. Mott RT, Ait-Ghezala G, Town T, Mori T, Vendrame M, Zeng J, Ehrhart J, Mullan M, Tan J: Neuronal expression of CD22: novel mechanism for inhibiting microglial proinflammatory cytokine production. *Glia* 2004, 46:369–379
 35. Cardona AE, Pioro EP, Sasse ME, Kostenko V, Cardona SM, Dijkstra IM, Huang D, Kidd G, Dombrowski S, Dutta R, Lee JC, Cook DN, Jung S, Lira SA, Littman DR, Ransohoff RM: Control of microglial neurotoxicity by the fractalkine receptor. *Nat Neurosci* 2006, 9:917–924
 36. Glass JD, Nash N, Dry I, Culver D, Levey AI, Wesselingh S: Cloning of m-calpain 80 kD subunit from the axonal degeneration-resistant WLD(S) mouse mutant. *J Neurosci Res* 1998, 52:653–660
 37. Bernier B, Castejon S, Culver DG, Glass JD: Axonal neurofilaments are resistant to calpain-mediated degradation in the WLD(S) mouse. *Neuroreport* 1999, 10:1423–1426
 38. Tsao JW, Paramanathan N, Parkes HG, Dunn JF: Altered brain metabolism in the C57BL/Wld mouse strain detected by magnetic resonance spectroscopy: association with delayed Wallerian degeneration? *J Neurol Sci* 1999, 168:1–12
 39. Koegl M, Hoppe T, Schlenker S, Ulrich HD, Mayer TU, Jentsch S: A novel ubiquitination factor, E4, is involved in multiubiquitin chain assembly. *Cell* 1999, 96:635–644
 40. Lehnardt S, Massillon L, Follett P, Jensen FE, Ratan R, Rosenberg PA, Volpe JJ, Vartanian T: Activation of innate immunity in the CNS triggers neurodegeneration through a Toll-like receptor 4-dependent pathway. *Proc Natl Acad Sci USA* 2003, 100:8514–8519
 41. Campbell IL, Abraham CR, Masliah E, Kemper P, Inglis JD, Oldstone MB, Mucke L: Neurologic disease induced in transgenic mice by cerebral overexpression of interleukin 6. *Proc Natl Acad Sci USA* 1993, 90:10061–10065
 42. Bettelli E, Das MP, Howard ED, Weiner HL, Sobel RA, Kuchroo VK: IL-10 is critical in the regulation of autoimmune encephalomyelitis as demonstrated by studies of IL-10- and IL-4-deficient and transgenic mice. *J Immunol* 1998, 161:3299–3306
 43. Brewer KL, Bethea JR, Yezierski RP: Neuroprotective effects of interleukin-10 following excitotoxic spinal cord injury. *Exp Neurol* 1999, 159:484–493
 44. Araki T, Sasaki Y, Milbrandt J: Increased nuclear NAD biosynthesis and SIRT1 activation prevent axonal degeneration. *Science* 2004, 305:1010–1013
 45. Wang J, Zhai Q, Chen Y, Lin E, Gu W, McBurney MW, He Z: A local mechanism mediates NAD-dependent protection of axon degeneration. *J Cell Biol* 2005, 170:349–355

46. Zhai Q, Wang J, Kim A, Liu Q, Watts R, Hooper E, Mitchison T, Luo L, He Z: Involvement of the ubiquitin-proteasome system in the early stages of Wallerian degeneration. *Neuron* 2003; 39: 217–225
47. Shimura H, Hattori N, Kubo S, Mizuno Y, Asakawa S, Minoshima S, Shimizu N, Iwai K, Chiba T, Tanaka K, Suzuki T: Familial Parkinson disease gene product, parkin, is a ubiquitin-protein ligase. *Nat Genet* 2000; 25:302–305
48. Saigoh K, Wang YL, Suh JG, Yamanishi T, Sakai Y, Kiyosawa H, Harada T, Ichihara N, Wakana S, Kikuchi T, Wada K: Intragenic deletion in the gene encoding ubiquitin carboxy-terminal hydrolase in gad mice. *Nat Genet* 1999; 23:47–51
49. Gillingwater TH, Wishart TM, Chen PE, Haley JE, Robertson K, MacDonald SH, Middleton S, Wawrowski K, Shipston MJ, Melmed S, Wyllie DJ, Skehel PA, Coleman MP, Ribchester RR: The neuroprotective *WldS* gene regulates expression of PTTG1 and erythroid differentiation regulator 1-like gene in mice and human cells. *Hum Mol Genet* 2006; 15:625–635
50. Gold BG, Voda J, Yu X, McKeon G, Bourdette DN: FK506 and a nonimmunosuppressant derivative reduce axonal and myelin damage in experimental autoimmune encephalomyelitis: neuroimmunophilin ligand-mediated neuroprotection in a model of multiple sclerosis. *J Neurosci Res* 2004; 77:367–377
51. Kanwar JR, Kanwar RK, Krissansen GW: Simultaneous neuroprotection and blockade of inflammation reverses autoimmune encephalomyelitis. *Brain* 2004; 127:1313–1331
52. Bjartmar C, Wujek JR, Trapp BD: Axonal loss in the pathology of MS: consequences for understanding the progressive phase of the disease. *J Neurol Sci* 2003; 206:165–171
53. Coles AJ, Wing MG, Molyneux P, Paolillo A, Davie CM, Hale G, Miller D, Waldmann H, Compston A: Monoclonal antibody treatment exposes three mechanisms underlying the clinical course of multiple sclerosis. *Ann Neurol* 1999; 46:296–304
54. Kornek B, Storch MK, Bauer J, Djamshidian A, Weissert R, Wallstroem E, Steffler A, Zimprich F, Olsson T, Linington C, Schmidbauer M, Lassmann H: Distribution of a calcium channel subunit in dystrophic axons in multiple sclerosis and experimental autoimmune encephalomyelitis. *Brain* 2001; 124:1114–1124
55. Brand-Schreiber E, Werner P: Calcium channel blockers ameliorate disease in a mouse model of multiple sclerosis. *Exp Neurol* 2004; 189:5–9
56. Black JA, Dib-Hajj S, Baker D, Newcombe J, Cuzner ML, Waxman SG: Sensory neuron-specific sodium channel SNS is abnormally expressed in the brains of mice with experimental allergic encephalomyelitis and humans with multiple sclerosis. *Proc Natl Acad Sci USA* 2000; 97:11598–11602
57. Pitt D, Werner P, Raine CS: Glutamate excitotoxicity in a model of multiple sclerosis. *Nat Med* 2000; 6:67–70
58. Araújo Couto L, Sampaio Narciso M, Hokoc JN, Blanco Martinez AM: Calpain inhibitor 2 prevents axonal degeneration of opossum optic nerve fibers. *J Neurosci Res* 2004; 77:410–419
59. Badalamente MA, Hurst LC, Stracher A: Calcium-induced degeneration of the cytoskeleton in monkey and human peripheral nerves. *J Hand Surg [Br]* 1986; 11:337–340
60. Wang MS, Wu Y, Culver DG, Glass JD: Pathogenesis of axonal degeneration: parallels between Wallerian degeneration and vincristine neuropathy. *J Neuropathol Exp Neurol* 2000; 59:599–606